60p.

File
NA55-809
N64-15191
CODE-1
CR-55644

Alkaline Battery Division

GULTON INDUSTRIES, INC.

Metuchen, N. J.

i. DESIGN, DEVELOPMENT AND MANUFACTURE

OF STORAGE BATTERIES FOR FUTURE

SATELLITES *Quarterly ... No 9, 4 Nov. 1962 –*
#9 4 Feb. 1963

Report No. 9

NATIONAL AERONAUTICS AND SPACE ADMINISTRATION *NASA* CONTRACT NO. NAS 5-809

(NASA CR-55644) OTS

NINTH QUARTERLY PROGRESS REPORT

4 November 1962 to 4 February 1963

Prepared By:

H. N. Seiger
Asst. Director of Research

H. Cohen   *1963 60 p*
Physical Chemist

Approved By:

R. C. Shair
Director of Research

GULTON INDUSTRIES, INC.
Alkaline Battery Division
Metuchen, New Jersey.

TABLE OF CONTENTS

LIST OF TABLES

LIST OF FIGURES

LIST OF FIGURES

Cont'd.

I. ABSTRACT

The twenty-five VO-50 HS hermetically sealed nickel-cadmium cells have been fabricated, completely checked out, and shipped to Goddard Space Flight Center.

VO-6 HS cells on a 50% depth continuous 90 minute period cycle have reached cycle number 2825 and the cycling continues.

The theories which have been propounded to explain the mechanism of the reduction of oxygen at the cadmium electrode in sealed nickel-cadmium batteries have been reviewed and critically examined. The most strongly propounded theory is that of a peroxyl ion mechanism. From the information we have at our disposal, we conclude that the peroxyl mechanism cannot be uniquely substantiated, and in fact, there is definite evidence against it. We have therefore proposed another mechanism which fits all the available data, and describe experimental work directed at substantiating this proposed mechanism.

Cell efficiency studies were conducted at relatively low temperatures and charge rates, by determining (1) the charge input necessary for gas evolution, (2) the self-discharge rate of the positive after charge, and (3) the recombination rate after oxygen pressurization. At low temperatures, the order of dependency of charge input required for gas initiation upon charge rate was inverted when compared with the order for the same rates at higher temperatures. The self-discharge rates doubled for a two-fold increase in charge rate and for a 40 - 50° rise in temperature. The recombination rates appeared to increase with temperature. *Author*

II. 50 A.H. HERMETICALLY SEALED CELLS

Production of the prototypes of the VO-50 HS cell is completed. To date, 25 cells have been shipped.

Performance has been excellent with capacities averaging 56 ampere-hours. Because of the nature of the larger seal and cover assembly, some difficulties were experienced initially in cell assembly. With some modifications in mechanical parts, the assembly techniques have been greatly improved.

Table I shows the complete electrical performance of the VO-50 HS cells shipped to Goddard Space Flight Center for evaluation and test.

TABLE I.

TEST HISTORIES OF GULTON VO-50 H.S.

HERMETICALLY SEALED CELLS FOR

N A S A

CELL NUMBER	OVERCHARGE FOR 24 HOURS AT 5.0 AMPS. VOLT.	PRESS.	ON CYCLE FOR 10 CYCLES CONSISTING OF: 36 MINUTE DISCHARGE AT 20.0 AMPS. 64 MINUTE CHARGE AT 13.5 AMPS. ON CYCLE PRESSURE	OVERCHARGE FOR 24 HOURS AT 5.0 AMPS. VOLT.	PRESS.	DISCHARGED AT 25.0 AMPS. TO 1.0 V PRESS.	A.H.	OVERCHARGE FOR 24 HOURS AT 5.0 AMPS. VOLT.	PRESS.	DISCHARGED AT 25.0 AMPS TO 1.0 V PRESS.	A.H.	SHORTED FOR 16 HRS: CHARGED 5 MINUTES AT 5.0 AMPS ON OPEN CIRCUIT STAND FOR 24 HOURS O.C.V.	OVERCHARGE FOR 24 HRS. AT 5.0 AMPS. VOLT	DISCHARGE AT 25.0 AMP TO 1.0 V. A.H.	OVERCHARGE FOR 24 HRS. AT 5.0 AMP. VOLT	DISCHARGED AT 25.0 AMP. TO 1.0 V. A.H.
100	1.40	39	5	1.39	35	-14	59.20	1.40	46	-10	59.17	1.19	1.42	60.83	1.41	60.83
101	1.40	41	4	1.39	41	-19	58.90	1.40	50	-20	58.91	1.19	1.42	61.08	1.41	61.26
102	1.40	63	13	1.38	59	-10	56.67	1.40	39	-15	56.25	1.20	1.40	58.34	1.41	58.75
103	1.40	60	13	1.38	54	- 5	59.17	1.40	39	-12	59.58	1.20	1.40	60.00	1.41	61.26
104	1.40	47	7	1.39	44	- 9	58.34	1.40	19	-20	58.34	1.20	1.40	59.58	1.41	60.00
107	1.42	49	6	1.38	22	3	56.67	1.38	40	5	55.00	1.17	1.39	61.68	1.39	59.17
108	1.43	15	-25	1.38	18	-29	63.34	1.38	22	-25	62.51	1.18	1.40	66.26	1.39	64.18
109	1.41	30	-2	1.38	25	- 8	58.34	1.38	23	- 5	56.25	1.16	1.40	61.26	1.39	59.17
111	1.41	35	0	1.38	31	- 9	58.76	1.38	30	- 2	56.67	1.17	1.40	62.09	1.38	60.01
115	1.42	46	2	1.38	38	5	57.51	1.38	38	- 2	55.42	1.19	1.40	60.43	1.38	58.76
116	1.41	39	0	1.40	31	-15	61.25	1.41	38	-14	62.45	1.20	1.40	62.08	1.40	62.91
117	1.40	39	- 5	1.39	31	-17	57.08	1.41	33	-15	58.33	1.18	1.39	59.58	1.39	60.00
118	1.41	31	- 5	1.39	26	-15	61.63	1.41	32	-12	62.08	1.19	1.39	62.81	1.39	62.08
119	1.41	23	- 5	1.39	26	-15	57.50	1.41	20	-12	58.33	1.18	1.39	60.00	1.39	59.58
120	1.41	25	- 8	1.39	20	-15	56.25	1.41	22	-12	56.67	1.18	1.39	57.50	1.39	59.58
121	1.41	24	- 8	1.39	21	-15	57.91	1.41	28	-14	58.75	1.18	1.39	59.58	1.39	60.41
123	1.40	28	- 8	1.39	21	-15	58.33	1.41	34	-12	59.58	1.18	1.40	60.41	1.39	61.66
124	1.41	30	- 5	1.41	26	-15	59.16	1.41	27	-14	60.00	1.18	1.40	60.41	1.40	61.66
125	1.41	30	- 5	1.39	24	-12	60.83	1.41	36	-12	61.66	1.19	1.39	61.66	1.39	62.08
126	1.40	25	- 8	1.39	21	-13	57.50					1.18	1.40	59.58		
127	1.40	15	-18	1.39	15	-22	58.48					1.18	1.40	61.25		
128	1.40	34	- 7	1.39	32	-10	59.16					1.18	1.40	62.08		
129	1.40	22	-12	1.39	17	-12	58.48					1.19	1.40	61.25		
130	1.40	20	-12	1.39	25	-12	60.00					1.17	1.40	62.08		
131	1.40	20	-11	1.39	23	-12	58.48					1.18	1.40	60.41		

3.

III. ELECTRICAL PERFORMANCE OF VO-6HS CELLS

A set of VO-6 HS cells was placed on automatic cycling on August 20, 1962, at a 50% depth of discharge, and a 90 minute cycle. This cycle consists of a 35 minute discharge at 5.15 amperes followed by a 55 minute charge at 3.86 amperes, which corresponds to an 18% overcharge based on capacity removed. A typical plot of cycle number 2825 is shown in Figure 1.

Figure 2 is a plot of the end-of-charge and end-of-discharge voltages versus cycle number. These are average valves calculated each day. There is a downward trend in the end-of-discharge voltage point, but a slight adjustment in the cycling current should rectify this. The end-of-charge voltage have stayed about 1.53 for the last 8000 cycles. Testing will continue on the same 90 minute cycle.

The three experimental VO-6 HS cells that remained on cycle at a 70% depth and a 90 minute cycle, and had completed 1500 cycles, were taken off cycle shortly thereafter. At cycle 1587 one of the cells dried out and failed during the weekend. The remaining two cells developed high pressure since the balance of charge-discharge current was upset. These cells had been on a 35 minute discharge at 7.2 amperes and a 55 minute charge at 5.5 amperes or a 20% overcharge. One cell failed, the other two were discharged at a lower rate and charged at a higher rate, resulting in high pressure.

IV. FUNDAMENTAL STUDY OF THE REDUCTION OF OXYGEN AT THE CADMIUM ELECTRODE

When oxygen is consumed in a fuel cell, the potential of the electrode is approximately -.02 volts versus the Hg/HgO, KOH electrode.[1] The oxygen consumption reaction in the nickel-cadmium battery occurs at the cadmium electrode at a potential of -0.90 volts versus the Hg/HgO, KOH electrode.

The potential -0.90 volts is that of the cadmium electrode which is tabulated in Latimer[2] as -0.80 volts[*], the difference being that the Hg/HgO, KOH electrode is about 0.1 volt more positive than the basic hydrogen electrode.[3]

Because the potentials at which the reduction of oxygen occurs in these two systems is so different, one is led to suspect that the mechanisms may be as different as the potentials. Also, the electrode material upon which a reaction is occurring may have specific catalytic effects. For instance, two oxygen reduction waves were found at the dropping mercury electrode in 7.2M aqueous potassium hydroxide. No such waves were observed, however, at a rotating gold electrode.[4] Instead, with small cathodic polarization, a maximum in current was observed similar to that observed by Breiter[5] during the reduction of oxygen adsorbed on Pt by dissolved hydrogen.

An understanding of the mechanism governing the reduction of oxygen at the cadmium electrode is pertinent because this reaction is operative in the hermetically sealed nickel-cadmium cell. Basically, one needs

---

1. J. E. Wynn, Paper delivered at E.C.S. Meeting, Detroit, 1961.

2. W. Latimer, Oxidation Potentials, Prentice Hall, N. J., 1952.

* The signs in this report are based on the Gibbs-Stockholm Convention.

3. M. Barak, et alia, Paper delivered at E.C.S. Meeting, Detroit, 1961.

4. Gulton Industries, Inc., Signal Corps, 6th. Quarterly Report, Contract No. DA 36-039 SC-85390 Dec. 1961.

5. M. Breiter, J. Electrochem. Soc. 109, 425 (1962)

to know whether the reaction is rate controlled by oxygen transfer, or by the electrochemical process. Application of this knowledge will result in a greater overcharge capability.

It is important to note how such commercial cadmium electrodes are fabricated. A nickel powder having a density of approximately unity (the metal itself has a density of 8.9) is sintered upon a conductive grid. The grid is usually nickel or nickel plated cold rolled steel. The porosity of the sintered mass is in the order of 80%. Cadmium salts are impregnated into the sinter and converted into cadmium hydroxide. The resultant porosity after processing is reduced to approximately 50%. Thus, the cadmium electrode is to be regarded as a bielectrode consisting of an inert metal electrode and the $Cd/Cd(OH)_2$ electrode.

It is well-known that a charged Cd electrode removed from the electrolyte and held in air ignites while drying out. It is also well-known that a vented type cell that contains a one-way valve in a flexible case becomes concave several days after charge. This concavity is presumed due to a reaction between the atmosphere within the cell and the electrodes, particularly the negative electrode. It should be noted that hydrogen and oxygen are evolved from such cells and will sweep out the air.

Jeanine[6] reported that sintered nickel electrodes, not containing active material, closely spaced evolved less than the theoretical quantities of gases.

Neumann and Gottesmann[7] reported that oxygen is transferred by the gas phase and provided for "electrolyte free gas passages" in the separator, but neglected to provide a method for determining their presence.

6. R. A. Jeanine, Patent 2,646,455, July, 1953.

7. G. Neumann and V. Gottesmann, U.S. Patent 2,571,927, Oct. 1951.

Baars[8] put forth a theory that included both gaseous transport of oxygen, or, in the case of small interelectrode distances, a bridge which constitutes a short circuit of such magnitude as to support the current and the existing (it is presumed) pressure in the cell. These shorts were to burn themselves out on current interruption. This theory was later abandoned by Baars[9] in favor of a peroxyl mechanism similar to that of Berl[10] for the fuel cell oxygen electrode. It should be noted that Baars did not report an experimental finding of peroxide. Fleischer[11] using the sensitive titanate test was not able to detect peroxide.

Following Baars, Dehmelt and von Dohren[12] concur in a peroxide mechanism theory. Again, no direct experimental evidence was found to demonstrate peroxides formed in the cell while oxygen was being reduced. The strongest argument in favor of this mechanism was that the potential of their unimpregnated sinter became more positive when the oxygen pressure was increased, as happens with the fuel cell oxygen electrode.

Baars separated the function of the Cd metal and the nickel sinter in an ingeniously simple manner. He merely immersed Cd under electrolyte and "floated" a sintered nickel mass on top of the electrolyte. These two electrodes were connected through an ammeter. When oxygen was reaching the nickel mass, current flowed. In another experiment, having two unimpregnated nickel sinters closely spaced but separated by an electrolyte moistened separator, conducted in an atmosphere of oxygen, he was able to show that current could be passed without a change in oxygen pressure. Baars concluded that the reaction was electrochemical in nature,

8. E. Baars, Paper presented at the Electrochem. Soc. Meeting, Boston, 1954.

9. E. Baars, Proceedings 12th. Annual Power Sources Conference.

10. W. Berl, Trans. Electrochem. Soc. 83, 253 (1943).

11. A. Fleischer, Private Communication.

12. K. Dehmelt and H. von Dohren, Proceedings 13th. Annual Power Sources Conf.

and that the reaction took place on metallic nickel sites.

Dehmelt and von Dohren[12] ran experiments with unimpregnated cathodes. They too observed the reaction occurring at nickel sites. A cell was constructed in these laboratories consisting of nickel oxide electrodes and unimpregnated cathodes. During overcharging a substantially steady pressure was reached, indicating and agreeing with the previous investigators, that metallic Cd is not needed in a certain instance to effect oxygen reduction. The instance is overcharge. As will be seen later, however, metallic Cd is needed for the bulk of the pressure decay during open circuit.

Quintin and Viltange[13] conducted experiments with electropolished Ni immersed in electrolyte. Currents up to certain values for each interelectrode spacing could be passed without altering the oxygen pressure within the cell. They found two distinct regions which they feel correspond to a rapid diffusion of oxygen from the anode to cathode at small interelectrode spacings, region II. The other region, occurs when the electrodes are widely spaced so that the oxygen becomes gaseous, enters the gas phase and then redissolves in order to reach the cathode.

Recent Experiments - It is fairly difficult, in practice if not in principle, to run investigations on the oxygen reduction reaction in cells. The difficulty is due to the self-discharge of the positive electrodes which occurs at a substantial rate for approximately one-half to several hours (depending upon charge rate and temperature) following charge interruption. In spite of this inherent difficulty, some information on the reaction was obtained in cells[14], and were later confirmed by other workers in these laboratories.[15]

13. M. Quintin and R. Viltange, Compt rendu 250, 840 (1960)

14. Gulton Industries, Inc., Signal Corps, Final Report, June 1962,
    DA 36-039 SC-85390

15. Gulton Industries, Inc. AF Tec. Doc. Report No. ASD-TDR 62-67, April 1962.

It was shown that at oxygen pressures greater than about 2/3 at-mosphere the oxygen decay with time is semi-logarithmic. This indicates that the reaction is first order with respect to oxygen and zero order with respect to Cd. These observations were confirmed by even more direct exper-imentation. In some even more recent work, it was found that the region below 2/3 atmosphere is also semi-logarithmic, but additional efforts are needed to interpret the meaning of this finding.

Data were also obtained indicating that the specific heterogeneous rate constants during overcharge are greater.than the specific heterogeneous rate constants during open circuit.

Preliminary current-voltage studies indicate an absence of an oxygen wave at the cathodic nickel electrode[16]. Confirming this lack of a diffusion wave is the fact that the activation energy for the process is virtually independent of temperature[15]. Its value is 5.07 kcal per mole over the range of 25 to 40°C.

Discussion - The theories extant in the literature do not satisfactorily explain experimental observations made on cells and on negative electrodes. Let us first discuss the theory concerning short circuits. It would, indeed, be fortuitous for a "high resistance" short circuit to occur that will just compensate for the self-discharge of the positive electrodes, the voltage of the cells, and the gas pressure. More likely shorts may form that are intermittent. When the voltage starts to fall, the short will break. Under these circumstances one should be able to see the noise on an oscillo-scope. Such noise was not observed. It should be noted that noise would not be caused uniquely by shorts. Bubbles of gases forming on, and leav-ing the electrode would also cause noise. Consequently, the evidence does not indicate intermittent shorts, nor does it indicate gas bubble formation.

---

16. Unpublished data obtained in these laboratories

The peroxide theory, when set into the form of the Neinst equation, indicates a reaction that should be (1) first order with respect to oxygen, (2) zero order with respect to cadmium, (3) and at a constant current, make the electrode more positive when the oxygen pressure is increased. This theory does not of itself explain the apparent increased specific rate constant during overcharge, although it does predict the open circuit reaction at the cadmium electrode. Thus there are only two points which cause doubt to be established about this theory. One is the fact that peroxide was not found, and the second is that the polarization of the negative electrode is small[17] and in the wrong direction to account for a faster oxygen consumption during overcharge. If the earlier data is further substantiated, the lack of a peroxyl wave can not be explained in these terms.

Since the evidence is mounting[18] that the reduction of oxygen is indirect and activation controlled, the present theories are inadequate. A new theory has been promulgated and is presented in the next section.

Cathodic Oxygen Reduction Theory - An unpoised nickel electrode can cause the discharge of ions in solution when the potential is fixed. These discharged ions will be adsorbed on the surface of the electrode. Since an equilibrium is not set up with gases, the equilibrium is probably set up between the surface concentration of adsorbed gas and the concentration of the undischarged ions in solution. In this way the current associated with the change of potential is explained. If the applied potential is greater than the decomposition potential the surface will become saturated and gases will be evolved from the electrode.

---

17. Gulton Industries, Inc. Signal Corps Report, 4th. Quarterly, June, 1961
DA 36039 SC-35390

18. G. Bianchi, et alia, U.S. Government Research Reports AD 278690, abstract.

The fact that the negative electrode is a bi-electrode may now be used:

$$Cd, \ Cd(OH)_2/KOH \ (H^+, \ K^+, \ OH^-)/ \ H \circ Ni$$
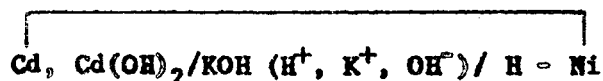
The line connecting the Cd to the Ni represents a short circuit as it exists in the system. That is, a mixture of Cd and Cd $(OH)_2$ is contained in the pores of the electrode which is sintered nickel. The electrolyte, aqueous KOH, covers both the Cd, Cd $(OH)_2$ mixture and the exposed nickel.

Oxygen reaching the nickel surface at any point where nickel is covered by electrolyte reacts with the adsorbed hydrogen and thereby upsets the equilibrium between the surface coverage and the solution. But the Cd, Cd $(OH)_2$ electrode buffers the voltage, in a sense, and additional Cd is converted into Cd $(OH)_2$ while depositing H atoms on the nickel surface;

$$Cd \ + \ H_2O \longrightarrow Cd \ (OH)_2 \ + \ 2H^+ \ + \ 2e^-$$

$$2H^+ \ + \ 2e^- \ (Ni) \longrightarrow 2H \circ Ni$$
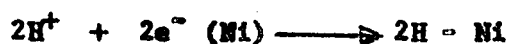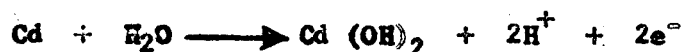
The reaction between oxygen and the adsorbed hydrogen is not represented since we have no concept, except a negative one, about the mechanism involved. Breiter[5] has shown that an electrochemical reaction between adsorbed oxygen and hydrogen exhibits a maximum rate at an intermediate potential. If the rate of this reaction is proportional to the surface area covered by oxygen, Θ, and to the surface area covered by hydrogen, $1-\Theta$, a maximum reaction rate would be observed when $\Theta = 0.5$. This has not been observed on Ni, although it was found on a gold electrode in 7.2N KOH. Therefore, there is still a lack of evidence concerning the mechanism of the reaction between hydrogen and oxygen at the surface.

Thus oxygen can be reduced at any place where the conditions are appropriate. During open circuit the reaction sites are elemental nickel

which is at the potential of the Cd, Cd $(OH)_2$ electrode and covered with a film of electrolyte. If we consider that the electrodes are closely spaced and the separator and electrodes are essentially saturated with electrolyte then the reaction sites are limited to the edge of the electrodes, the backs of the end electrodes and the tabs and terminals. The electrode faces covered by separator will represent a long path through which the oxygen must travel. It is much more likely for the reaction to occur through the shortest path[19] which is the film.

When a cell is placed on overcharge, oxygen can continue through the gas phase. In addition, with interelectrode distances of 0.2 mm. or less[13], oxygen can travel directly from the anode to the cathode, effectively increasing the number of reaction sites.

Required Experimental Proof - The theory given above will account for the observations made on sealed cells, on negative electrodes, and on unimpregnated electrodes.

At the pressures to which this theory is applicable it is readily understood why the rate is independent of the amount (or state-of-charge) of the negative electrode whether the electrode state-of-charge is altered by discharge or by reaction with oxygen. The reaction will occur at a rate proportional to the amount of oxygen at the metal/solution interface. The Cd, Cd $(OH)_2$ electrode, which does not polarize under these conditions, will merely replace the hydrogen removed.

The rate of the reaction will be dependent upon the number of sites, or electrode area, at which the reaction will occur. Thus it will be sensitive to the amount of electrolyte within the cell; more electrolyte will leave fewer film paths. Also, additional reaction sites will be available during overcharge if the interelectrode distance is small.

19. D.A. Sama, et alia, J. Electrochem. Soc. 109, 884 (1962)

A low activation energy merely means that the reaction can occur at a significantly rapid rate at low temperatures. The constancy of the activation energy over the 25 to 40°C range is not inconsistent with a chemical process.

While the theory proposed above does fit the observations drawn from many sources, certain proofs must be obtained. These proofs must be obtained under unquestionable and rigorous experimental conditions. Perhaps one of the most important of these proofs is a continued study of the current-voltage and current-time characteristics of nickel wire and porous nickel electrodes. These studies are to be made to study the effects of convection (natural convection is absent in zero G environment), the effects of porosity, and the effects of several oxygen partial pressures on these characteristics. These experiments were started during the past quarter and shall constitute the experimental section on this reaction.

Let us set up the chemical equations that correspond to the reactions of this theory;

$$1) \quad H^+ \; + \; e^- \; \xrightarrow{\; i \;} \; H(M)$$

$$2) \quad O_2 \; + \; 4H(M) \; \xrightarrow{\; k \;} \; 2H_2O.^*$$
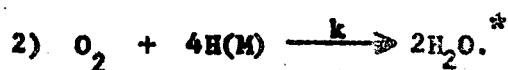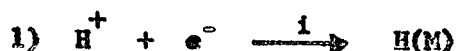
Equation 1 is merely the electrochemical process of discharging a proton which is adsorbed on the electrode. The rate at which this process proceeds is given by the current i. This process will occur only with current, that is, it commences with current flow and ceases with interruption as in any electrochemical process. Equation 2 is a chemical process that will proceed at a rate dependent only upon the surface concentration of adsorbed atoms and the partial pressure of oxygen. If the rate at which the process represented by equation 2 proceeds is slower than the rate at which that represented by equation 1 proceeds, then two predictions can be made. The

---

* Equation 2 does not purport to represent a mechanism, but merely gives the overall process. Equation 1 is mechanistic.

first prediction is that there will be a lag in oxygen consumption before the steady oxygen consumption rate is reached. This corresponds to the deposition of H atoms on the nickel surface. The second prediction is that oxygen will continue to be consumed after current interruption. This corresponds to a depletion of the hydrogen already on the Ni. These predictions will be an especially pertinent test of the theory proposed herein.

Another set of proofs would be the investigation of pressure as a function of the amount of electrolyte. Several attempts were made previously, but are unreliable since the state-of-charge of the electrode is altered when the cell is vented. Although the gas phase reaction is unaffected by the state-of-charge, there is a possibility that the more dense Cd allows more reaction sites to be available on the electrode surfaces covered by the separator and electrolyte. It has already been found that a cell can be made to perform sealed even when the negative electrode has taken all the charge it can accept. It is expected that this experiment can be run while overcoming this complication. Therefore, cells deficient in electrolyte will be prepared. They will be fully charged vented. They can then be evacuated and oxygen put in just before the cells are returned to charge. When steady pressures are obtained, additional electrolyte can be added, and oxygen to replace that lost, can be put into cell.

The third set of proofs, which has already been done, is to fabricate flooded sealed cells. Since oxygen can be transported through the solution according to the theory, and based on the current-voltage curves and Quintin and Viltange's observations[13], one can predict that flooded sealed cells can be made operable. Since oxygen is being generated at the anode and this goes into solution, some must go into the gas phase in accordance with Henry's Law. While this is occurring, the amount of oxygen reach-

ing the cathode will be insufficient to prevent charging. Consequently hydrogen will be evolved. If one waits long enough for the appropriate gradients to evolve, and vents the cells to purge the hydrogen then sealed flooded cells should be made. Groups of 4 to 5 such cells were made on three occasions. This constitutes sufficient proof of their preparation, and helps substantiate the theory.

Experimental - The polarization circuit consisted of a transformer which steps up the AC to 350 volts. This was rectified through a 6×4 vacuum tube, filtered and regulated to 105 volts with an OB2 mercury vapor voltage regulator. The output was then stepped down through a resistor and a Zener diode (Motorola Catalogue No. 1M2.4AZ) which supplied a regulated 1.5 volts. A Spectral Model 810 ten turn precision linear potentiometer having a resistance of 100 ohms was connected across the Zener diode. A 1 rpm synchronis motor was used to drive the potentiometer through a 1:1 gear train.

A shunt was placed in the positive leg of the circuit. This shunt was a General Radio Decade Resistance Box. The current was read on the Y coordinate of a Mosely Model 2A X-Y recorder. The recorder was always set on its most sensitive range (5mV full scale) so that the potentiometric feature of the instrument could be used. (See Figure 3)

The positive electrode, the counter electrode, was a 0.005 inch platinum foil having a relatively large geometric surface area, 63.0 cm^2.

The negative terminal of the power supply was connected to the test electrode.

A mercury, mercuric oxide/KOH half-cell was used to determine the cathode potential. The potential was recorded on the X coordinate of the X-Y recorder. The reference electrode was connected to the system using a Luggin capillary.

The electrolyte used was identical with that employed in the hermetically sealed nickel-cadmium cell, 34% aqueous potassium hydroxide.

Electrode Preparation - Grade B nickel wire of 0.0589 cm. diameter was sealed into a soft glass tube. The exposed length of wire was cut to 1 cm. leaving a geometric surface area of 0.19 cm^2.

The electrode was mechanically cleaned to remove the blackened oxides caused by heat sealing into glass. It was degreased in acetone and air dried. Nitric acid cleansing did not permit the current-voltage curves to be reproducible, and this treatment was abandoned.

The initial runs, cathodic polarizations, were not reproducible. After two runs, the subsequent cathodic polarizations are very reproducible. Between runs, the electrode was kept on open circuit until it reaches the potential that it had in the previous run.

The porous electrode was cut from an unimpregnated sinter. The dimensions were 1 cm. by 1/2 cm. The termination was the nickel plated steel tab. The edges of the electrode were coated with polystyrene dissolved in methyl ethyl ketone in order to stop-off the exposed steel grid edges. This electrode was degreased in acetone prior to application of this stop-off lacquer. This edge-coating process is identical with that used in cells. The sintered electrode also requires one or two preliminary cathodic polarization before subsequent runs are reproducible. However, the sintered electrode does not require a waiting period before the next run is made.

The nickel wire electrode was rotated at 600 rpm in several experiments using a Sargeant Synchronous Rotator.

To sweep out all gas which may interfere, tank nitrogen was used as a purge. The end of the tubulation contained a sintered glass gas dispersion tube. Experiments with air (P_{O_2} = 0.2 atm.) were done by

attaching a compressed air line to the gas dispersion tube. Experiments with oxygen were carried out using tank oxygen gas. All experiments were done at room temperature (27° to $28^{\circ}C$).

Results - The current-voltage curves (polarograms) of Ni wire microelectrode obtained in a relatively oxygen-free electrolyte are shown in Figure 4. The electrolyte was purged with N_2 for 15 minutes prior to each run, but the purging was stopped just before the run was started. This particular run was reproducible and the figure is only one example of the data obtained. Other examples, in which the voltage was not driven above 1.0 volt are shown in Figure 5. The zero has been displaced in the three sets of data shown in Figure 5.

The lowest curves in Figure 5 represent the initial run, and it can be seen that these results are not in agreement with the other two in Figure 5, nor with the results in Figure 4.

At the potential of the Cd, Cd $(OH)_2$ electrode, -0.90 volts (obtained by a direct measurement), the average current at the unstirred electrode is 39.5 ± 1.3 uA/cm^2. When the electrode is rotated at 600 rpm, the current at the same potential increases to 43.3 ± 2.6 uA/cm^2.

In Figure 6 the current-voltage curves for the sintered nickel electrode are shown. The upper and lower curves indicate the reproducibility obtained. Qualitatively, these polarograms for the sintered electrode are similar to those obtained at the solid wire electrode. That is, they do show a typical activation controlled type process. Quantitatively there are differences between the two kinds of electrodes. At -0.90 volts, the current through the electrode is 406 ± 31 uA/cm^2. The area is based on geometric area. This is 9.4 times greater than on the wire electrode. At -0.8V the current at the sinter is 188 ± 25 uA/cm^2. The ratio in this

case is 38. These differences may merely be due to the fact that the data is obtained in a transitory manner, polarographically.

The effect of oxygen on the stationary microelectrode was determined during the past quarter. These results are shown in Figure 7. The lowest curve represents the same kind of results as shown in Figures 4 and 5. In the earlier runs stirring was achieved with a motor, while in this run agitation was achieved by vigorously bubbling nitrogen through the solution with the aid of a gas dispersion tube. Note that the current at -0.90 volts are in good agreement.

The run in which the partial pressure of oxygen is at 0.2 atmospheres was obtained by introducing compressed air into the solution. The current density increased, at the potential of interest, from 47 to 50 uA/cm^2.

When the solution is saturated with oxygen at a partial pressure of one atmosphere, the current is increased to 60 uA/cm^2.

Discussion of Results - During the past quarter the apparatus was set up as indicated. The apparatus was modified until it was possible to obtain data without unwarranted polarization of the reference electrode.

The data reported are, of course, only the first results obtained. The shape of the curves for the electrolyte saturated with oxygen at 1 atmosphere does not indicate an oxygen wave. Instead, the presence of oxygen merely increases the current at these potentials in which we are interested. These observations are consistent with the theory presented earlier. It should also be noted, that if one looks at Figure 7 in a different manner, the observations of Dehmelt and von Dohren[12] are also in evidence. If the current is kept constant, which we can perceive by using a current tie line between the curves in Figure 7, as the oxygen pressure is raised the potential becomes more anodic.

Convection has but a small influence on the currents in these measurements.
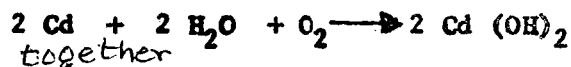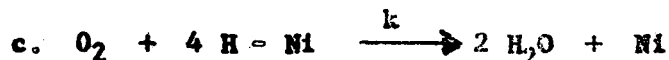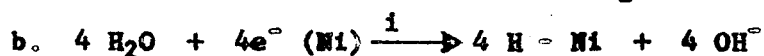
NOTE ADDED IN PROOF:

The equation 1,

$$H^+ + e^{\circ} \; (Ni) \longrightarrow H \circ Ni,$$
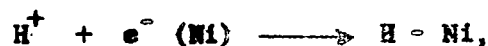
is better written according to Potter[20] as

$$H_2O + e^{\circ} \; (Ni) \longrightarrow H \circ Ni + OH^{\circ}$$

Thus the mechanism proposed will consist of three steps as follows:

a. $2 Cd + 4 OH^{\circ} \overset{i}{\longrightarrow} 2 Cd(OH)_2 + 4e^{\circ}$

b. $4 H_2O + 4e^{\circ} \; (Ni) \overset{i}{\longrightarrow} 4 H \circ Ni + 4 OH^{\circ}$

c. $O_2 + 4 H \circ Ni \overset{k}{\longrightarrow} 2 H_2O + Ni$

_____

$$2 Cd + 2 H_2O + O_2 \longrightarrow 2 Cd(OH)_2$$

Reactions a and b, *together*, is a corrosion reaction so that the current i shown as the rate is the corrosion rate, not the charge rate. When a cell is overcharged the corrosion rate may or may not be altered. If it is altered, then reaction b will have a corrosion current different from that of reaction a, that is: $i_b \geq i_a$. Thus the state of charge of the negatives can remain unaltered while the chemical reaction C is not directly affected by the current i_b, but is merely affected by the partial pressure of oxygen and the degree of surface coverage of the Ni matrix by hydrogen atoms.

_____

20. E. C. Potter, Electrochemistry, Cleaver ‑ Hume, London, 1956.

V. CHARGE EFFICIENCY STUDIES

Introduction - This phase of the work is concerned with the understanding of charge efficiency of sealed nickel-cadmium cells at temperatures below $77^\circ F$. The experiments performed during the eighth quarter were designed for charge at constant current. For work at cold temperatures during this last quarter, cells were also charged at controlled potential. In this method, the cells are charged by a power supply which (through a sensing circuit that is preset to some desired value) tends to maintain the cell voltage at a fixed potential after the current requirements fall within the capabilities of the charger. At the beginning of charge the current surges to a value consistent with the cell resistance and polarization, and then falls with time to some assymptotic value. This method lends itself very well to low temperature work because (1) the cell voltage is limited, and (2) a great deal of charge may be put into the cell before the current falls to a low value which may be safe enough for continued overcharge without the production of high gas pressures. However, the surge current may be too high to permit safe charging, so that a series resistor is often introduced into the circuit to limit the surge current. In this case, the charge proceeds at a current fixed by the resistor for a time depending upon the cell polarization. After this, the current decreases to some low value. The resistor is only effective at high currents; at low currents, the voltage drop across the resistor is negligable. This was the method employed in the work to be described.

Experimental Procedures -

1. Low Temperature Charge Efficiency Studies at Constant Current

The six ampere-hour sealed cells which were employed in the high temperature charge efficiency experiments were used in the present tests.

The cells were divided into groups containing three cells which were brought to temperatures of -15°, 0°, 25°, and 50°F. At each temperature, one cell was charged at one of the selected rates which were 0.6A, 0.3A, and 0.15A. During each charge, the changes in cell pressure were noted. The charges were continued until the cells reached a pressure of 150 psig or achieved a steady state pressure. When one of these conditions was in evidence, each cell was tested for hydrogen by collecting a sample of gas and igniting it. A negative test meant that oxygen was present in large quantities.

At this point, each cell was evacuated and the charge was immediately interrupted. The course of the self discharge was followed by monitoring the cell pressure.

When this test was completed, the cells were pressurized to 50 psig of oxygen. The consequent pressure decay was monitored in the same manner as the self discharge.

After the pressure decay test, each cell was discharged at 3A to 1.0 volt for capacity.

2. Low Temperature Charge Efficiency Studies at Controlled Potential

Apparatus for controlled potential charging was assembled according to the circuit shown in Figure 8. The power supply employed was the Lambda Model L A100-03A, which is capable of supplying a regulated output of up to 34 volts at a current of 10 amperes.

Three 6 AH sealed nickel-cadmium cells (after being given four stabilization cycles as described in the 8th. report), were given a twenty-four hour stand in a cold box to reach 0°F. The cells were then charged at 1.55 and 1.60 volts respectively. Tests were made and data collected in the same manner as previously described for the constant current work (pressure rise during charge; pressure change during charged stand, and pressure decay).

Experimental Results

The pressure changes of the cells during charge have been plotted
for the various charge rates and temperatures, and are shown in Figures
6 - 9. At temperatures of 50° and $25^{\circ}F$ (Figures 9 and 10) the charge input
for initiation of gas evolution decreased with increase in charge rate and
decrease in temperature, as found in the high temperature test results
given in the previous report. However, as the temperature is further de-
creased, first to $0^{\circ}F$ (Figure 11) and then to $-15^{\circ}F$ (Figure 12), the order of
dependence on charge rate for the onset of gas evolution is inverted. The
charge input required for initiation of gas evolution _increases_ as the
charge rate is increased at these low temperatures. As the temperature is
decreased, the input for the onset of gas evolution is also decreased. It
was noted also, that the gases in the various cells during charge, except
at the 0.15A rate at $50^{\circ}F$, were found to contain hydrogen, even when steady
state pressures were attained.

The charge input required to produce gas is plotted as a function
of charge current in Figure 13. The graph shows that the input to produce
gas varies considerably with charge rate and temperature. At 25° and $50^{\circ}F$,
progressively greater inputs are associated with the onset of gas evolu-
tion as the charge rate is decreased and the temperature is increased.
However, at 0° and $15^{\circ}F$, although the dependence of input for gas formation
upon temperature is the same as given above, the order according to rate
is reversed. The 0° and $15^{\circ}F$ isotherms show that progressively greater in-
puts are obtained as the charge rate is increased. This phenomenon indi-
cates that there is an inversion point between the 0° and 25° isotherms.
This inversion point is clearly shown in Figure 14, where the charge input
to start pressure rise is plotted versus temperature. The inversion temp-

erature is in the vicinity of $10^\circ F$.

The self-discharge curves obtained after charge interruption are given in Figures 15 - 18. Again, as was given in the Eighth Report, the "initial rates of pressure rise" increases with increasing temperature and also with charge rate, while the dwell time at the plateau decreases with increasing temperature. (See Table II)

The pressure decay data obtained after each cell was pressurized to 50 psig with oxygen are plotted in Figures 19 - 22. Although the data are somewhat scattered, an examination of these curves shows that the initial pressure decay rates appear to increase with temperature.

The cell capacities obtained after discharge at 3 A to 1.0 volt are listed on Table III.

The preliminary results obtained from 1.60 and 1.55 volt controlled potential charging at $0^\circ F$ are shown in Figures 23 and 24. The current-time curve plotted in Figure 20 for a 1.60 volt charge, is typical of this method, as described earlier. At any time t, the charge input Q is equal to the area under the curve up to that time, and is given by the expression:

$$Q = \int_{t=0}^{t=\tau} \dot{i}\, dt$$

The area under the curve was integrated using a planimeter.

The charge input required for gas evolution occurred approximately one ampere-hour earlier for the 1.60 volt charge, than for the charge at 1.55 volts.

In Figure 21 is shown the self-discharge curves obtained after charge at the two controlled potentials. These curves show that the self-discharge rate is higher for the 1.60 volt charge than for the charge at 1.55 volts.

TABLE II.

INITIAL RATES OF PRESSURE RISE DURING CHARGED STAND
INCHES OF MERCURY/MINUTE

Charge Rate Amperes	Temperature $^\circ$F			
	-15	0	25	50
0.15	0.25	0.33	0.50	.75
0.30	0.50	0.67	1.00	1.50
0.60	1.00	1.25	2.00	3.00

TABLE III.

CELL CAPACITIES AFTER 3 AMPERES DISCHARGE TO 1.0 VOLT

CHARGE RATE Amperes	TEMPERATURE, $^\circ$F, OF CHARGE (Discharge at Room Temperature, after 3 days stand)			
	-15	0	25	50
0.15	6.2	6.2	6.3	6.3
0.3	6.4	6.4	6.2	6.5
0.6	7.0	7.1	6.3	6.7

Discussion

The discussion in the Eighth Report indicated that two electrode reactions may be associated with charge efficiencies of less than unity. One is the oxidation of water at the positive to form oxygen, and the second is the reduction of water at the negative to form hydrogen. In addition, a third reaction - the formation of water as a consequence of oxygen reacting with hydrogen at the negative electrode - could serve to maintain the cell at some steady pressure. The occurrence of the first two reactions was in evidence throughout these tests, while the third was strongly suggested, in some cases, by the results obtained.

Consider Figures 9 - 12. At these lower temperatures, hydrogen is obtained, except for 50°F, where oxygen is found at the 150 ma rate and a mixture of hydrogen and oxygen is found at the 300 ma rate. At the low temperatures and relatively high charge rates hydrogen is evolved at the onset of pressure rise. This implies a decrease in charge efficiency for the negative electrodes under these conditions. In order to make conclusions about the positive electrodes with regard to efficiency, additional low rate constant current work at higher temperatures is needed, and will be performed during the next quarter. Of equal significance is the appearance of steady states with hydrogen, obtained for the first time in these tests. This shows that oxygen has reached the negative, as in the high temperature tests. One way to express this interaction between the positive and negative electrodes is to say that the positive is not inefficient enough to enhance depolarization of the negative. Another way of stating this concept would be (since predominantly hydrogen is produced as the temperature is lowered) to say that even at these low charge rates, the negative is first passivated and then depolarized.

The low temperature inversion phenomenon shown in Figure 11 indicates that the net effect of decreasing temperature and charge rate may serve to decrease the efficiency of the negative relative to that of the positive.

The results obtained during self-discharge (Figures 15 - 18) from the work reported here were similar to those obtained during the high temperature tests. The initial self-discharge rates tabulated in Table II indicate that these rates are charge dependent as well as temperature dependent. As the charge rate is doubled each step in going from 0.15 to 0.30 to 0.60 amperes, the decay rates also double, essentially for each current step. The initial self discharge rate approximately doubles for a 40 to $50^{o}F$ temperature rise.

The cell capacities in these tests do not, as was mentioned in the Eighth Report, give information regarding cell efficiency, since the charge input for each cell was different. These data are shown in Table III. These discharges were carried out at room temperature after a 3-day stand. At these lower temperatures the capacities still remain above 6 AH. It does appear that the lower the temperature the more effective is a higher charge rate. For instance, at 0° and $-15^{o}F$ the cells charged at 0.6 A yielded 7 AH at room temperature. This is reminiscent of the data in the previous report for 3 and 6 A charges at 77 and $90^{o}F$. In a sense, the meaning of a high charge rate depends upon temperature. At $77^{o}F$ the C/10 rate is not a high charge rate which it is at $0^{o}F$.

The quantity of experimental data is insufficient, at present, to give any analysis of cell behavior under controlled potential charge conditions. However, this work is being continued so that additional work will be available for evaluation in the next report.

VI. PROGRAM FOR NEXT PERIOD

The VO-6 HS cells on 50% depth continuous automatic cycle will continue in their cycle routine.

.   Further work will be done on the reduction of oxygen at the cadmium electrode. Details of the experimental work appear at the end of Section IV.

Details of the experimental work contemplated for the charge efficiency studies appear at the end of Section V.

Charge efficiency studies at controlled potential will be continued and completed.

Additional constant current charge at 0.15 and 0.3A at $77^{\circ}F$ and $90^{\circ}F$ will be made.

Additional polarographic studies will be made at the sintered electrode. Current time effects will also be measured.

The solutions at high O_2 concentration during cathodic polarization will be tested for H_2O_2.

It will be determined whether there is a lag in oxygen consumption upon commencement of cathodization, and whether oxygen consumption continues after current interruption.

VII. PERSONNEL

The following staff personnel worked on this project during the past quarter:

DR. R. C. SHAIR   DIRECTOR OF RESEARCH

DR. H. N. SEIGER   ASST. DIRECTOR OF RESEARCH

G. RAMPEL   SENIOR CHEMIST

J. LISKA   CHEMICAL ENGINEER

R. DAGNALL   MECHANICAL ENGINEER

A. LYALL   CHEMICAL ENGINEER

H. COHEN   PHYSICAL CHEMIST

FIGURE 1

CYCLING of VO-6HS CELLS

CYCLE NO. 2825, 50% DEPTH

35 MIN DISCHARGE, 5.15 AMPS
55 MIN CHARGE, 3.86 AMPS

CELL VOLTAGE

TIME MINUTES

M1444
AB 3000-9

FIGURE 2a

CYCLING of VO-6HS CELLS
90 MINUTE CYCLE - 50% DEPTH

CHARGE - 3.86 AMPS - 55 MINUTES
DISCHARGE - 5.15 AMPS - 35 MINUTES

END OVERCHARGE
VOLTAGE

END of CHARGE
END of DISCHARGE

CYCLES

FIGURE 2 b

CYCLING of VO-6HS CELLS
90 MINUTE CYCLE-50% DEPTH
CON'T (SHEET 2)

GULTON INDUSTRIES INC.   AB3000-9
METUCHEN, N. J.

M1269-2

CYCLES

END of CHARGE

END of DISCHARGE

FIG. 3   34.

M1499
AB 3000-9

D-1:	2.4 V ZENER DIODE
M :	0-1.5 VDC METER
T-1:	150V POWER TRANSFORMER
F-1:	FUSE, #3A SLOW BLOW
S-1:	SPST SWITCH
E :	Hg/HgO REFERENCE
V-1:	6 X 4 TUBE
V-2:	OB2 VR TUBE

C-1:	4 μf 450V
C-2:	20 μf 450V
R-1:	1.5 K, 1/2 W
R-2:	4 K, 1/2 W
R-3:	7 K, 1/2 W
R-4:	5 K, 2 W
R-5:	100 Ω 10 TURN POT
R-6:	RESISTANCE BOX,
	0-100 Ω

= CHASSIS GROUND

POLARIZATION CIRCUIT AND CELL SETUP FOR
CATHODIC POLAROGRAPHY

-1.5 VDC

R-4
R-3
R-2
R-1
V-1
V-2
C-1
C-2

R-5
D-1
M

T-1
F-1
S-1

TO "Y" INPUT
OF X-Y
RECORDER

R-6

TO "X"
INPUT OF
X-Y RECORDER

CELL
E

FIG. 4

35.

POLAROGRAMS OF NICKEL WIRE CATHODE NO. 1
IN 34% KOH, OXYGEN-FREE ELECTROLYTE
1. STATIONARY ELECTRODE
2. ROTATING ELECTRODE

CURRENT, MICROAMPERES

CATHODE VOLTS VS Hg/HgO, KOH

M1500
AB 3000-9

FIG. 5

POLAROGRAMS OF NICKEL WIRE CATHODE NO. 1
IN 34% KOH OXYGEN-FREE ELECTROLYTE
1, 3, 5 ROTATING CATHODE
2, 4, 6 STATIONARY CATHODE

CATHODE VOLTS VERSUS Hg/HgO, KOH

CURRENT, MICROAMPERES

M1501
AB 3000-9

EUGENE DIETZGEN CO
MADE IN U.S.A.

NO 340 20 DIETZGEN GRAPH PAPER
20 X 20 PER INCH

FIG. 6

37.
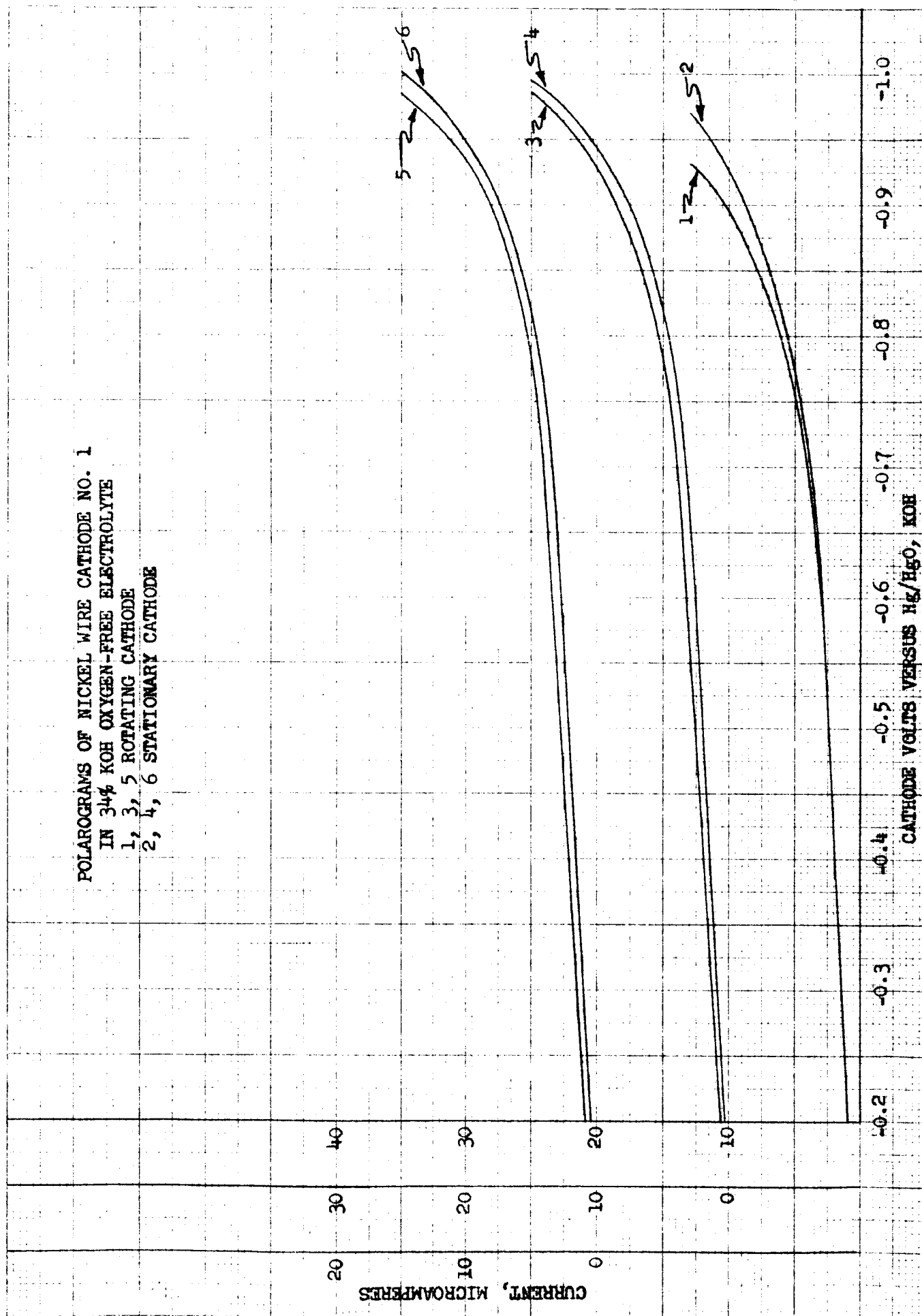
M1502
AB 3000-9

POLAROGRAMS OF SINTERED NICKEL CATHODE NO. 1
IN 34% KOH, OXYGEN-FREE ELECTROLYTE

CATHODE VOLTS VS Hg/AgO, KOH

CURRENT, MILLIAMPERES

EUGENE DIETZGEN CO.
MADE IN U.S.A.

N° 340 20 DIETZGEN GRAPH PAPER
20 X 20 PER INCH

FIG. 7

38.

POLAROGRAMS OF STATIONARY NICKEL WIRE CATHODE NO. 2
IN 34% KOH

1. TANK N_2 PURGE (O AT ATMOSPHERES O_2)
2. 0.2 ATMOSPHERE O_2 PURGE
3. 1. ATMOSPHERE O_2 PURGE

CURRENT, MICROAMPERES

CATHODE VOLTS vs H_2/H_gO, KOH
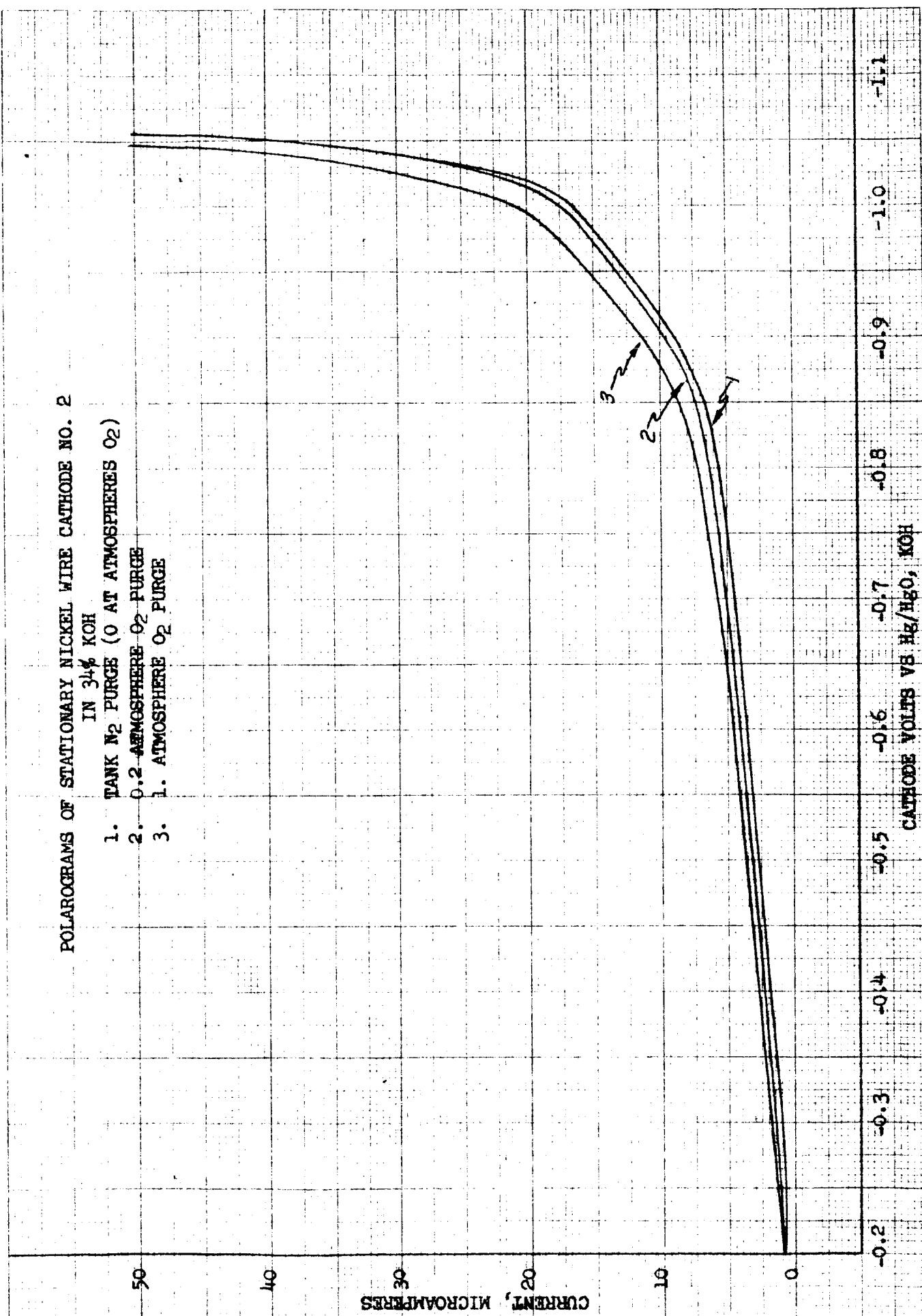
FIG. 8   39.

CIRCUIT FOR CONTROLLED POTENTIAL CHARGE
OF SEALED NI CD CELLS
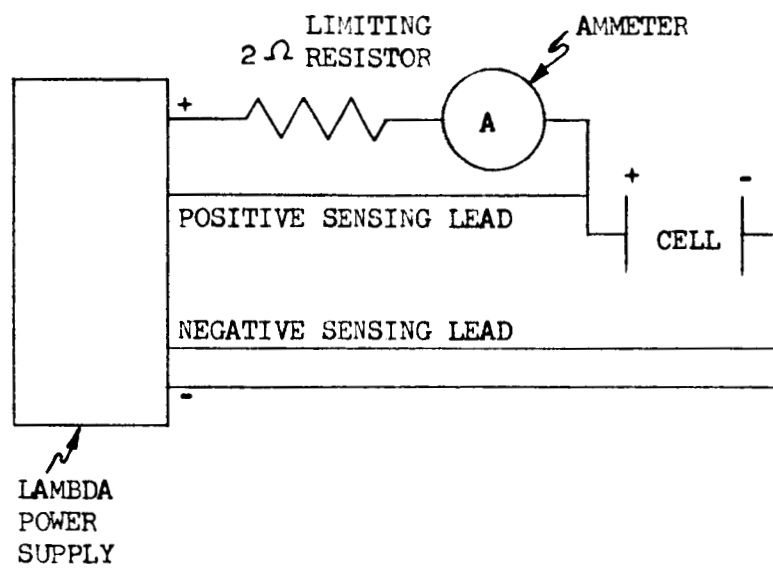
6 AH SEALED NICKEL-CADMIUM CELLS
PRESSURE RISE DURING CHARGE AT 50°F
● 0.6 A CHARGE
○ 0.3 A CHARGE
△ 0.15 A CHARGE

FIG. 10   41.
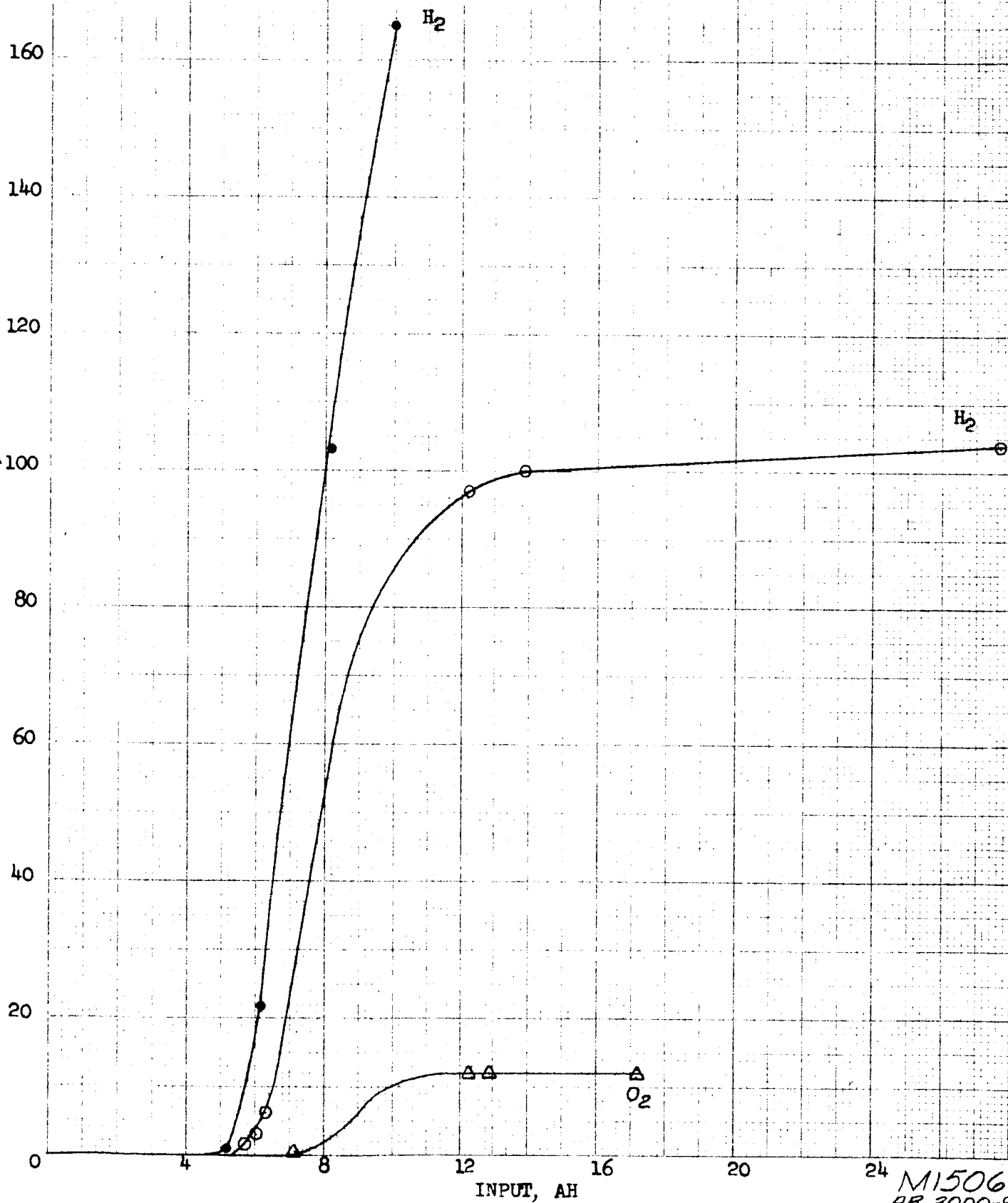
6 AH SEALED NICKEL-CADMIUM CELLS
PRESSURE RISE DURING CHARGE AT 25°F
• 0.6 A CHARGE
○ 0.3 A CHARGE
△ 0.15 A CHARGE

PRESSURE, PSI

INPUT, AMPERE-HOURS

M1507
AB 3000-9

FIG. II   42.

6 AH SEALED NICKEL-CADMIUM CELLS
PRESSURE RISE DURING CHARGE AT O°F
0.6 A CHARGE
0.3 A CHARGE
0.15 A CHARGE

M1508
AB 3000-9

FIG. 12   43.
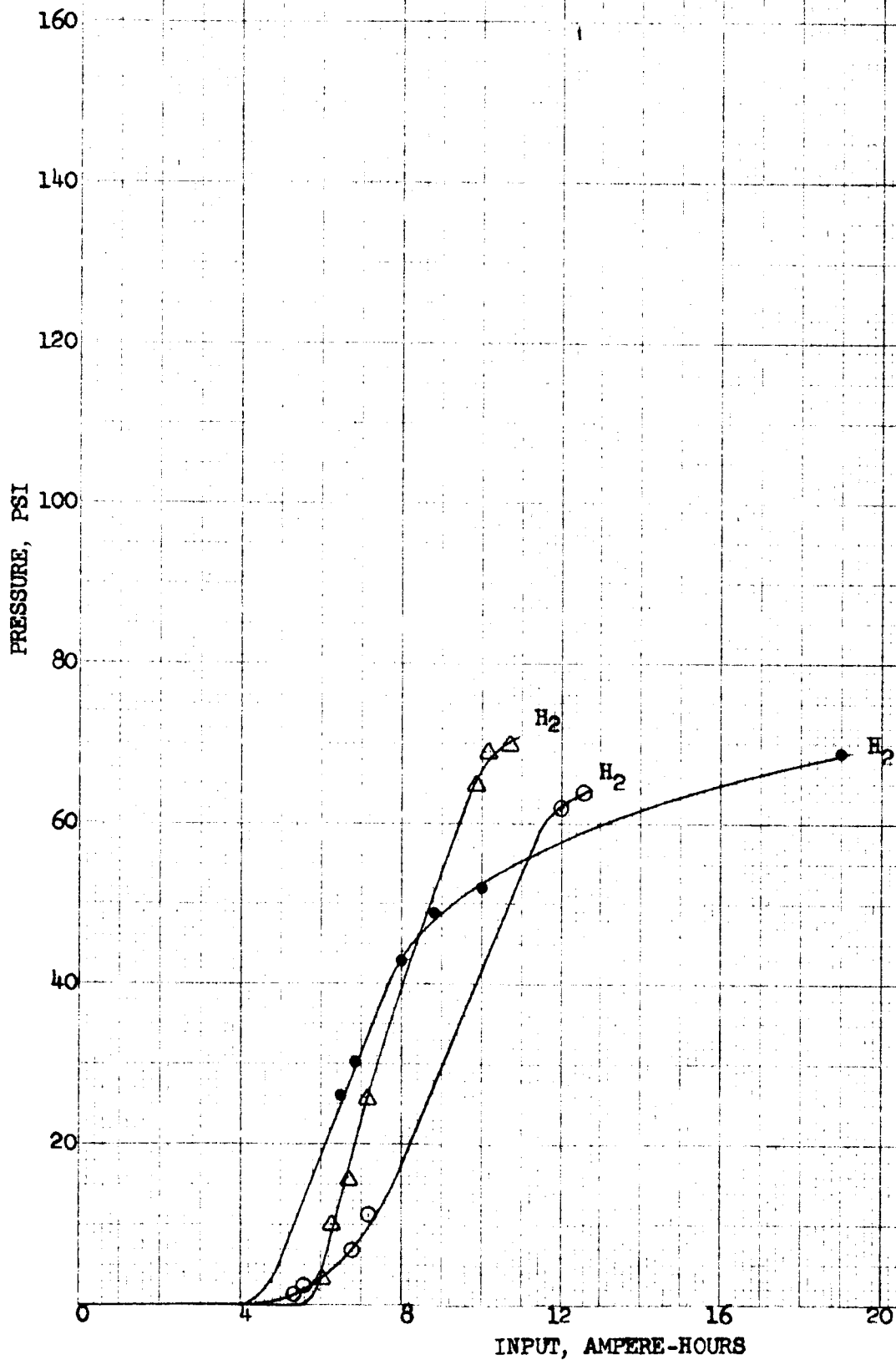
6 AH SEALED NICKEL-CADMIUM CELLS
PRESSURE RISE DURING CHARGE AT 0° F
0.6 A CHARGE
0.3 A CHARGE
0.15 A CHARGE
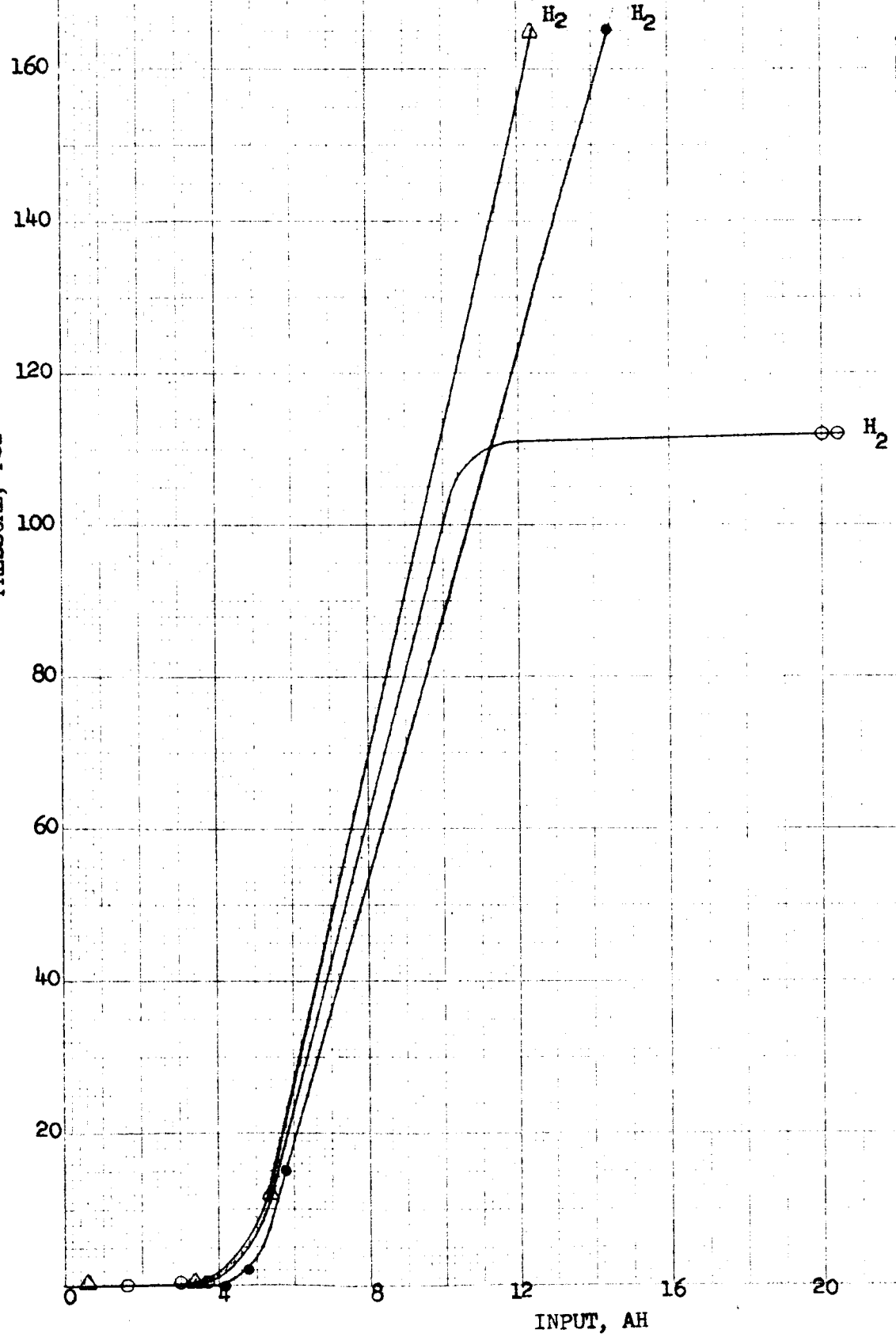
PRESSURE, PSI

INPUT, AH

EUGENE DIETZGEN CO.
MADE IN U.S.A.

NO. 340-20 DIETZGEN GRAPH PAPER
20 X 20 PER INCH

M1509
AB 3000-9

FIG. 13

6 AH SEALED NICKEL-CADMIUM CELLS:
CHARGE INPUT TO START PRESSURE RISE
AT VARIOUS TEMPERATURES

CHARGE INPUT, AMPERE HOURS

CHARGE CURRENT, AMPERES

- 0.6 A CHARGE RATE
- 0.3 A CHARGE RATE
- 0.15 A CHARGE RATE

FIG. 14

45.

6 AH SEALED NICKEL-CADMIUM CELLS:
CHARGE INPUT TO START PRESSURE RISE
AT VARIOUS TEMPERATURES

TEMPERATURE, °F

CHARGE INPUT, AMPERE-HOURS
TO START PRESSURE RISE

INVERSION POINT

◆ 6.0 A CHARGE
◇ 3.0 A CHARGE
▲ 1.2 A CHARGE
● 0.60 CHARGE
○ 0.30 CHARGE
△ 0.15 A CHARGE

M1511
AB 3000-9
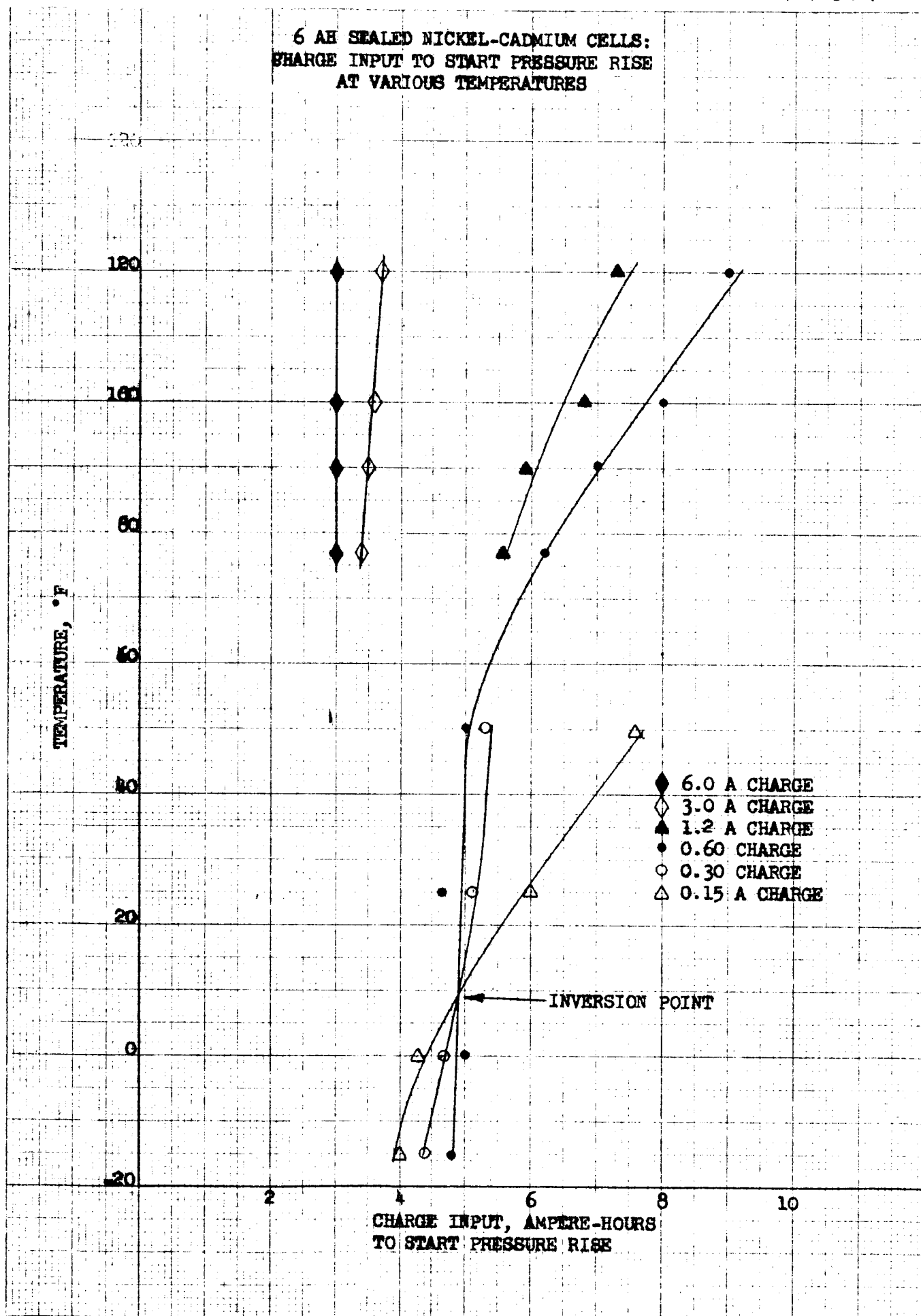
6 AH SEALED NICKEL-CADMIUM CELLS:
PRESSURE CHANGES DURING CHARGED STAND
AT 50° F

● 0.6 A CHARGE
○ 0.3 A CHARGE
△ 0.15 A CHARGE
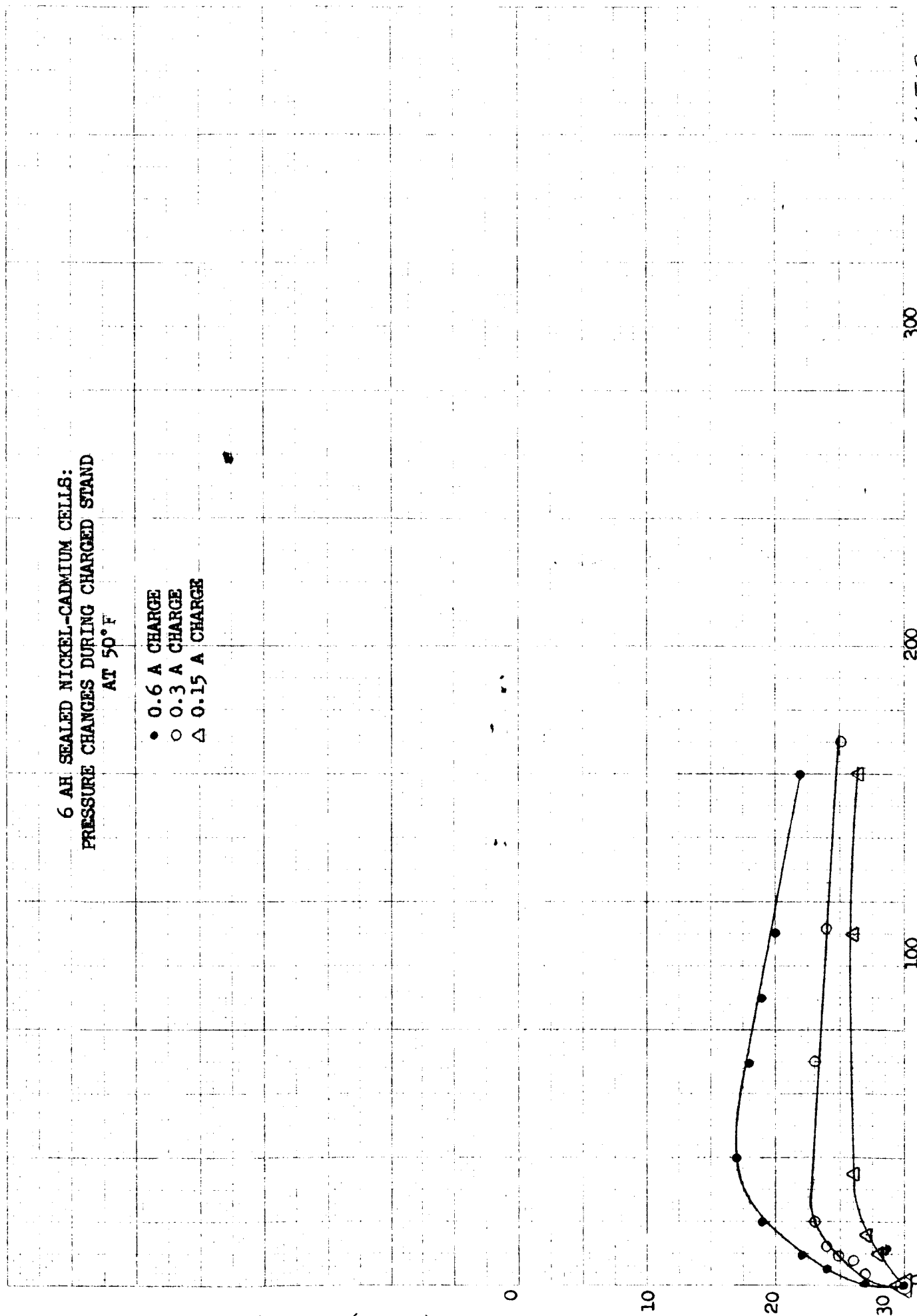
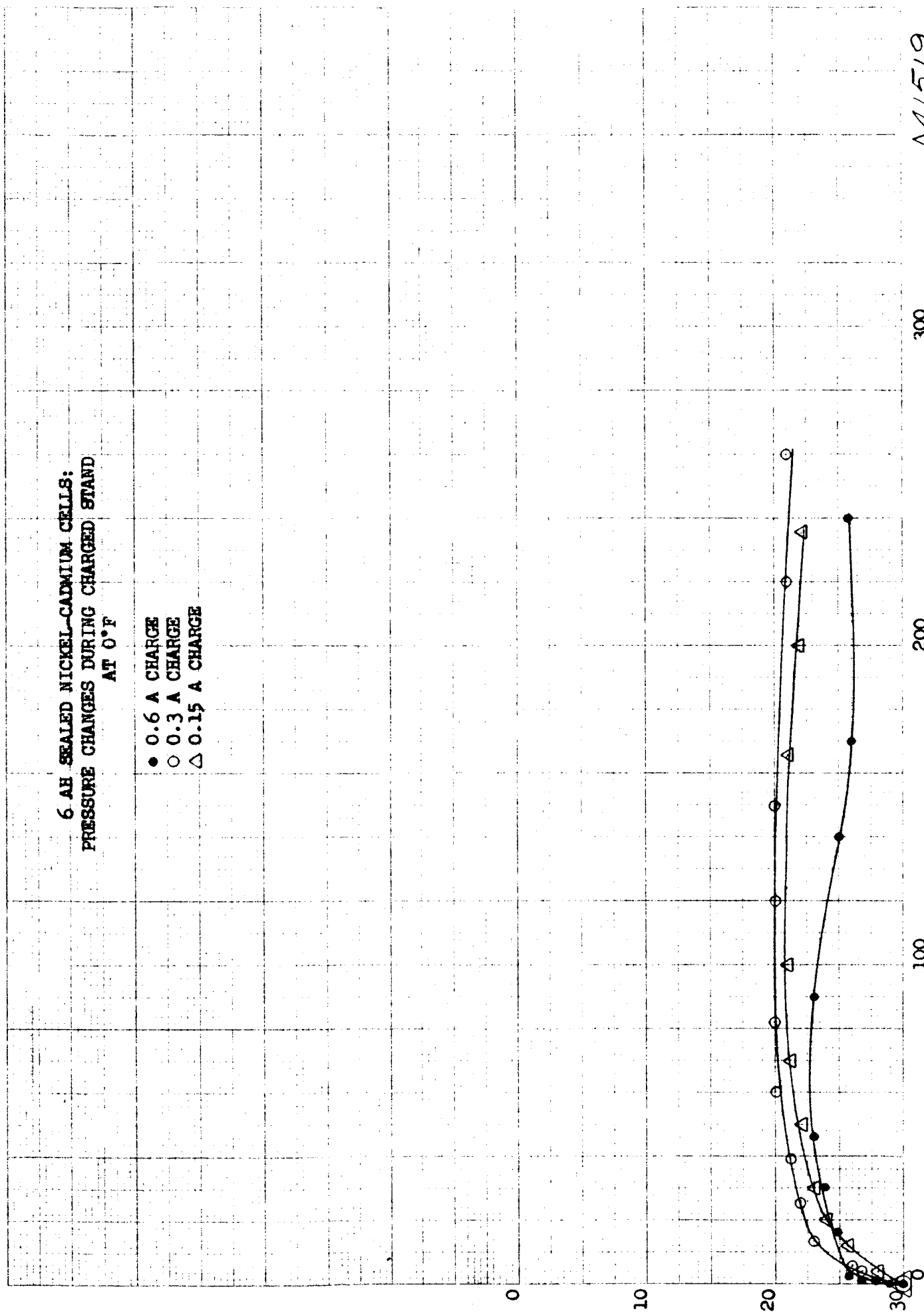PRESSURE (INCHES, MERCURY)

TIME (MINUTES)

FIG. 15

46.

M1512
AB 3000-9

6 AH SEALED NICKEL-CADMIUM CELLS:
PRESSURE CHANGES DURING CHARGED STAND
AT 25°F.

● 0.6 A CHARGE
○ 0.3 A CHARGE
△ 0.15 A CHARGE

PRESSURE (INCHES, MERCURY)

TIME (MINUTES)

FIG. 16

47.

M1513
AB 3000-9

FIG. 17

48.
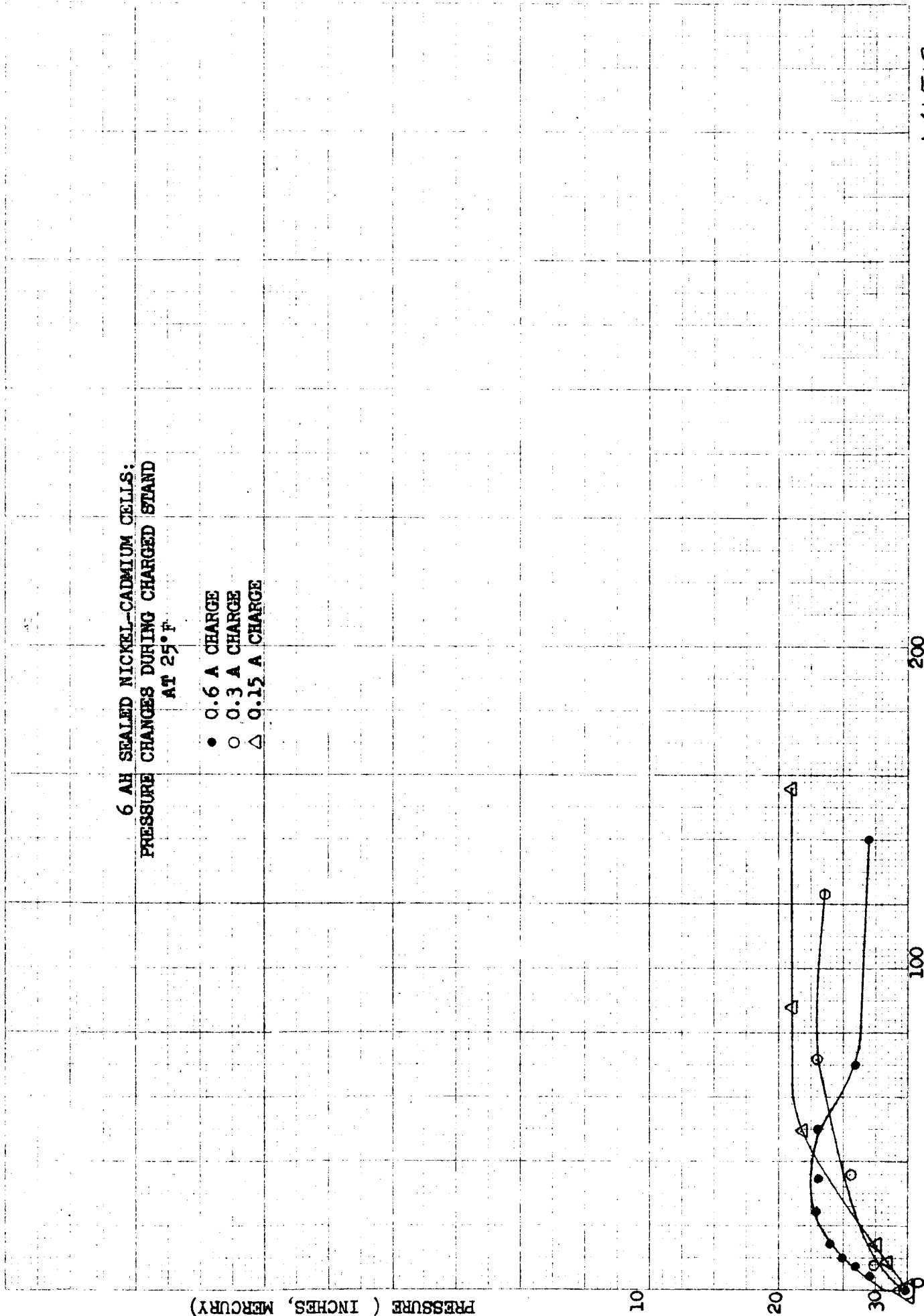
M1519
AE 3000-9

6 AH SEALED NICKEL-CADMIUM CELLS:
PRESSURE CHANGES DURING CHARGED STAND
AT 0°F

● 0.6 A CHARGE
○ 0.3 A CHARGE
△ 0.15 A CHARGE

PRESSURE IN MERCURY

TIME, MINUTES

6 AH SEALED NICKEL-CADMIUM CELLS:
PRESSURE CHANGES DURING CHARGED STAND
AT -15°F

● AFTER 0.6 A CHARGE
○ AFTER 0.3 A CHARGE
△ AFTER 0.15 A CHARGE

FIG. 18

49.

M1520-9
AB 3000-9

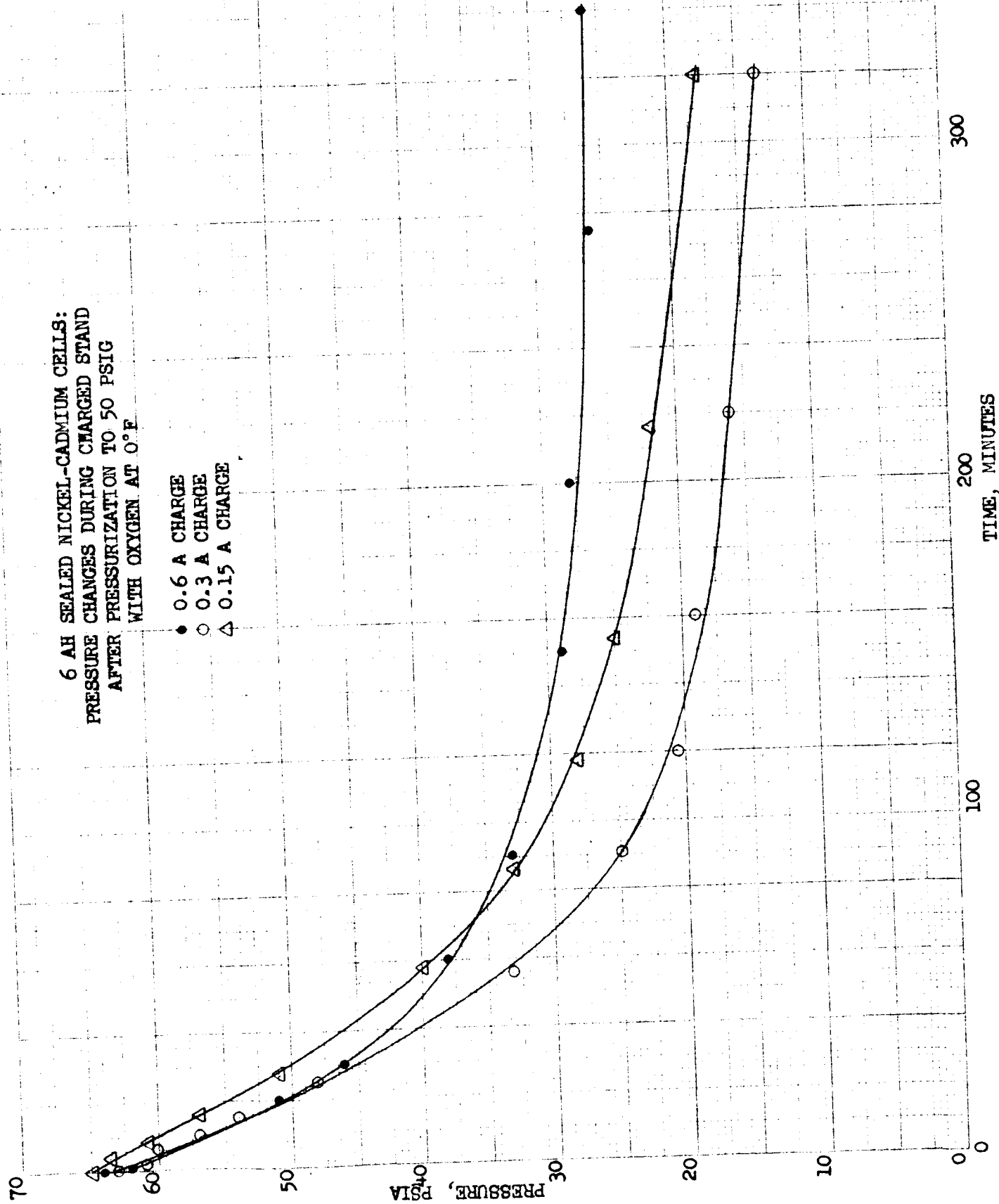TIME, MINUTES

PRESSURE, INCHES OF MERCURY

FIG. 19   50
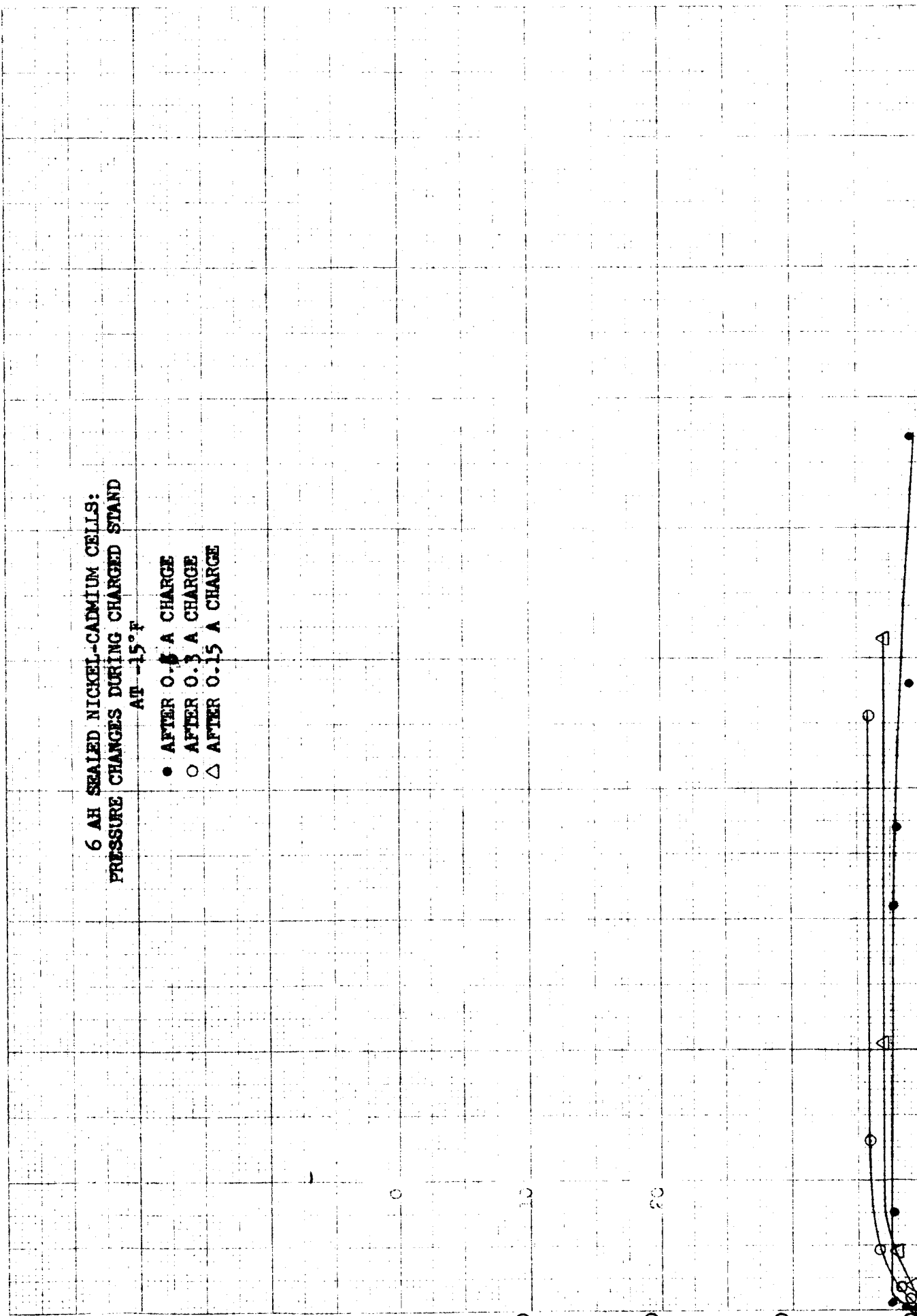
6 AH SEALED NICKEL-CADMIUM CELLS:
PRESSURE CHANGES DURING CHARGED STAND
AFTER PRESSURIZATION TO 50 PSIG
WITH OXYGEN AT -15°F

- 0.6 A CHARGE
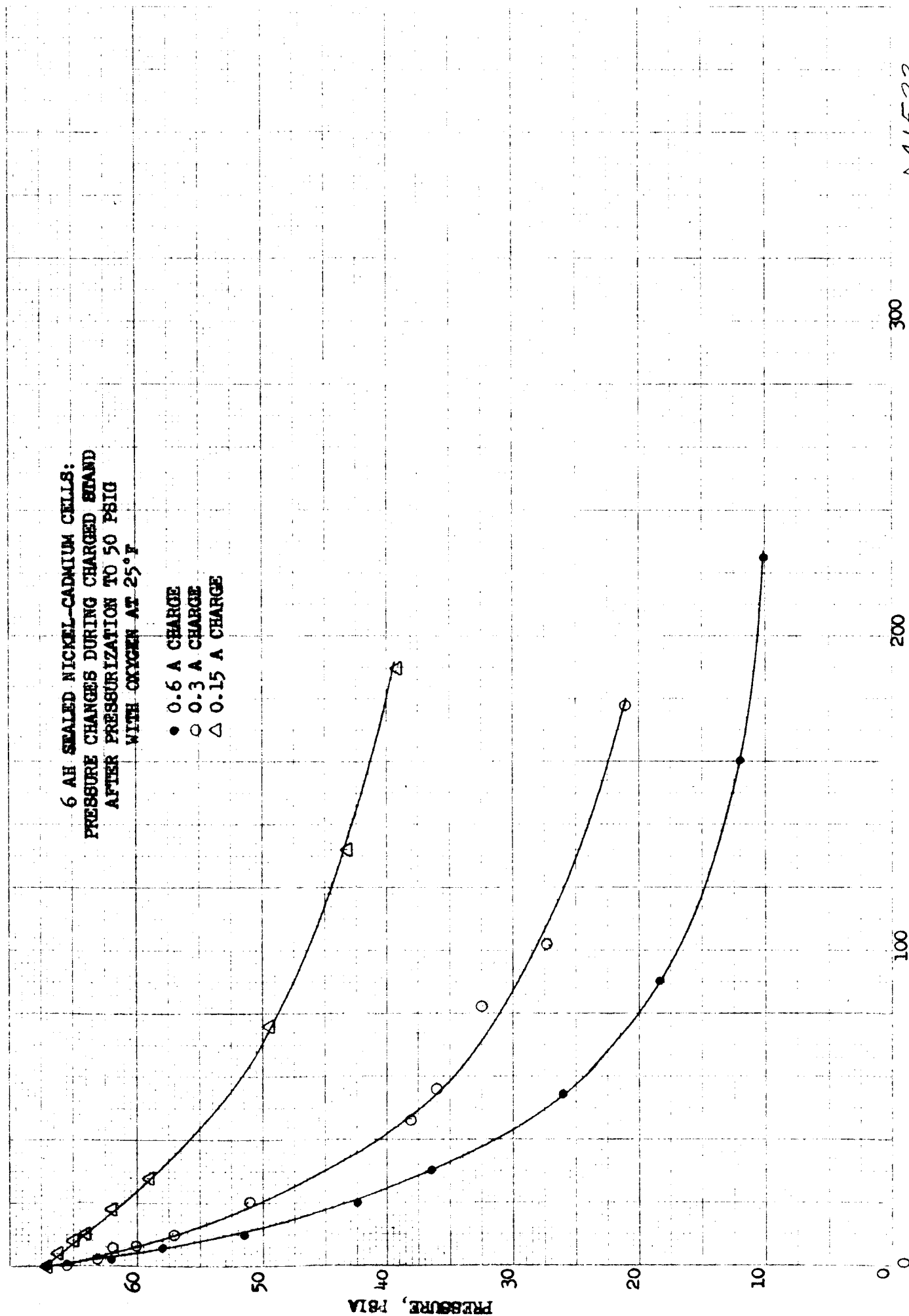○ 0.3 A CHARGE
△ 0.15 A CHARGE
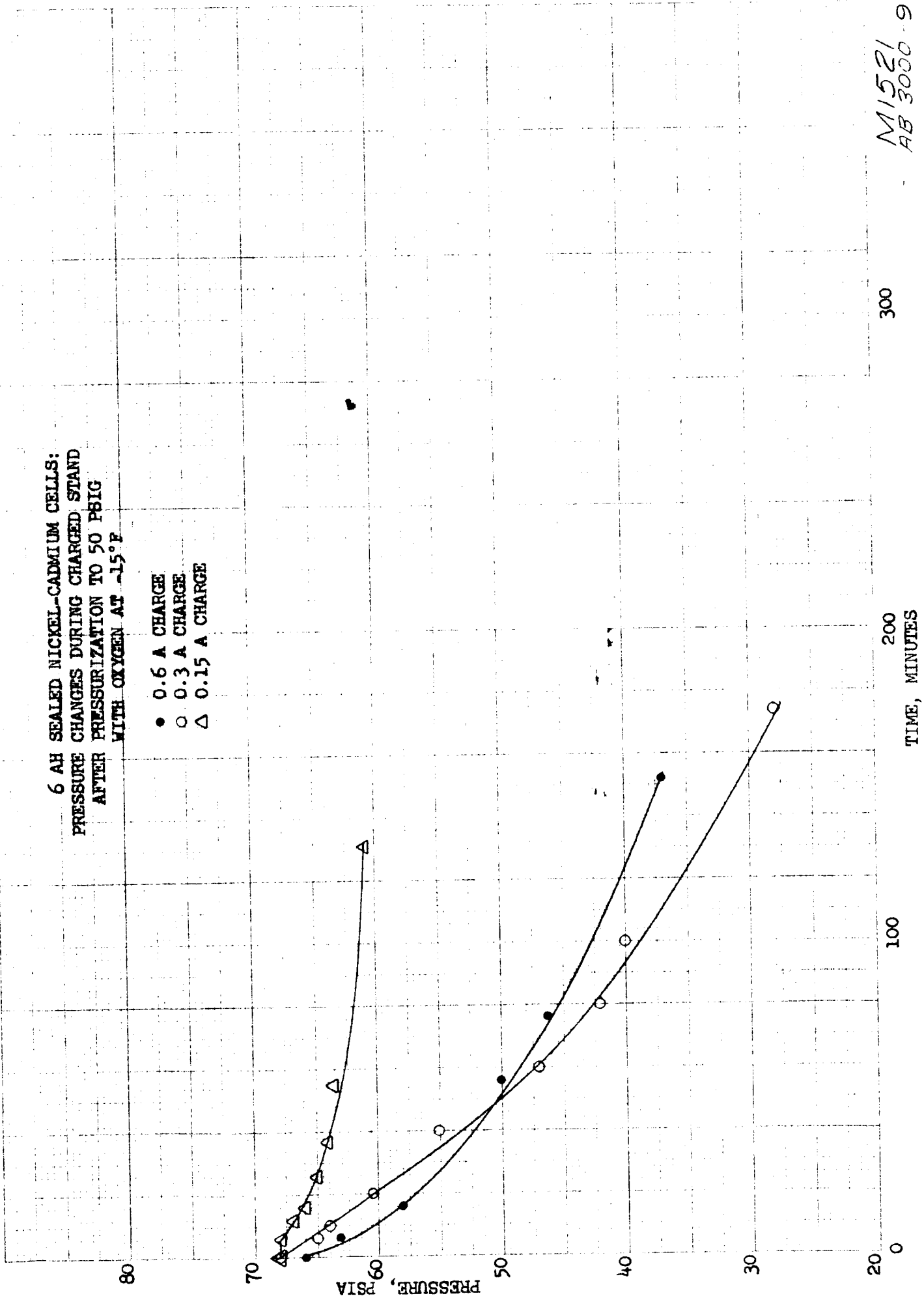
PRESSURE, PSIA

TIME, MINUTES

FIG. 20   51.

6 AH SEALED NICKEL-CADMIUM CELLS:
PRESSURE CHANGES DURING CHARGED STAND
AFTER PRESSURIZATION TO 50 PSIG
WITH OXYGEN AT 0°F

● 0.6 A CHARGE
○ 0.3 A CHARGE
△ 0.15 A CHARGE

FIG. 21

52.

.6 AH SEALED NICKEL-CADMIUM CELLS:
PRESSURE CHANGES DURING CHARGED STAND
AFTER PRESSURIZATION TO 50 PSIG
WITH OXYGEN AT 25°F

● 0.6 A CHARGE
○ 0.3 A CHARGE
△ 0.15 A CHARGE

FIG. 22

M1524
AB 3000-9

EUGENE DIETZGEN CO.
MADE IN U.S.A.

NO. 340-20 DIETZGEN GRAPH PAPER
20 X 20 PER INCH

6 AH SEALED NICKEL-CADMIUM CELLS:
PRESSURE CHANGES DURING CHARGED STAND
AFTER PRESSURIZATION TO 50 PSIG
WITH OXYGEN AT 50°F

● 0.6 A CHARGE
◇ 0.3 A CHARGE
△ 0.15 A CHARGE

TIME, MINUTES

PRESSURE, PSIA

FIG. 23

6 AH SEALED NICKEL-CADMIUM CELLS:
CONTROLLED POTENTIAL CHARGE CURVE AT
AT 1.60 VOLTS AND 0°F

FIG. 24

55.

M1526-9
AB 3000-9
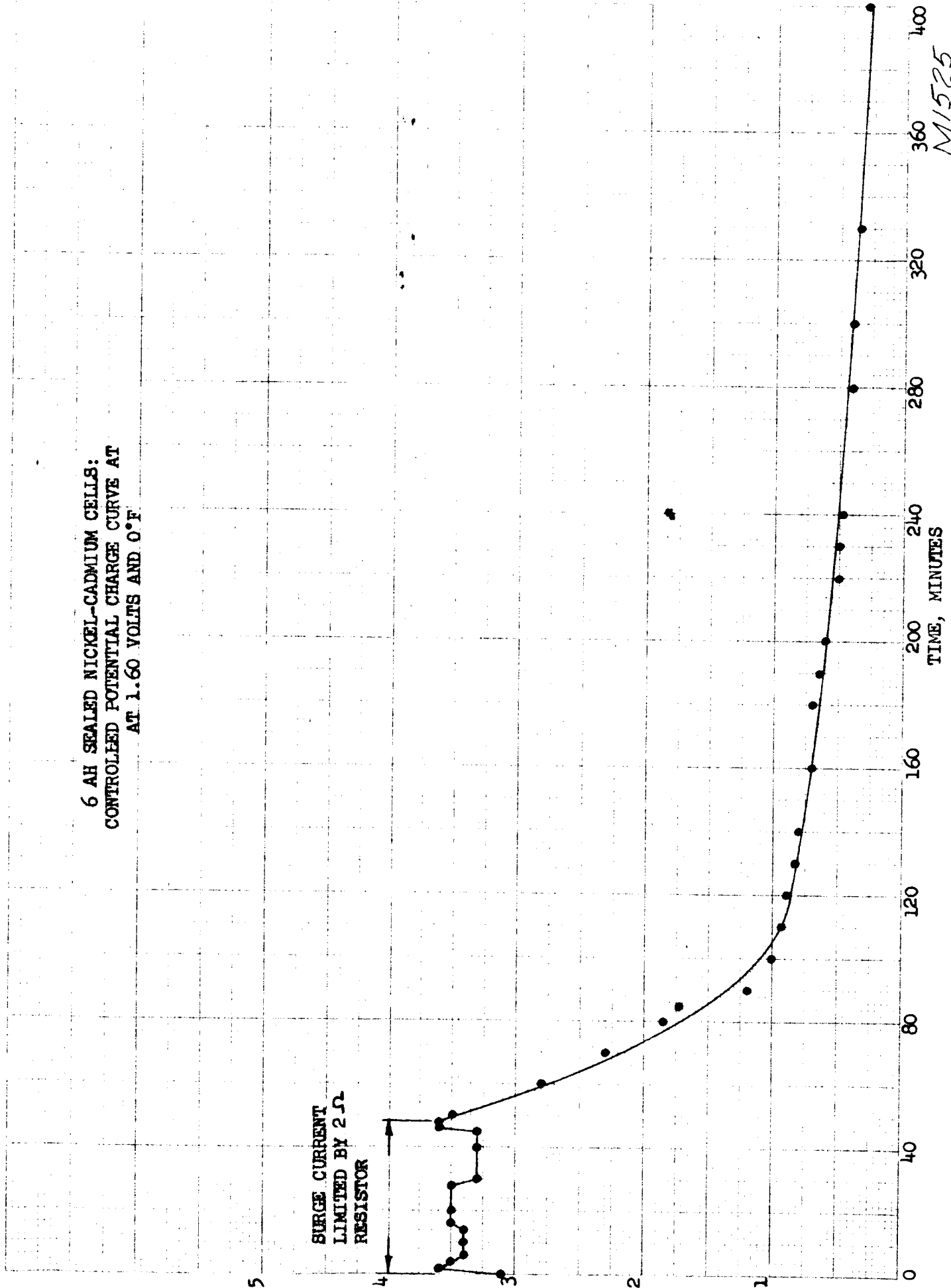
6 AH SEALED NICKEL-CADMIUM CELLS:
PRESSURE CHANGES DURING CHARGED STAND
AFTER CONTROLLED POTENTIAL CHARGE
AT 0°F

● EVACUATED AFTER 1.60 VOLT CHARGE
○ EVACUATED AFTER 1.55 VOLT CHARGE

TIME, MINUTES

GAUGE PRESSURE
INCHES OF MERCURY